Ion transport by nanochannels in ion-containing aromatic copolymers

Li, Nanwen; Guiver, Michael D.

Publisher's version / Version de l'éditeur:
https://doi.org/10.1021/ma402254h
Macromolecules, 47, 7, pp. 2175-2198, 2014-02-18

April 8, 2014
Volume 47
Number 7

Macromolecules

pubs.acs.org/Macromolecules

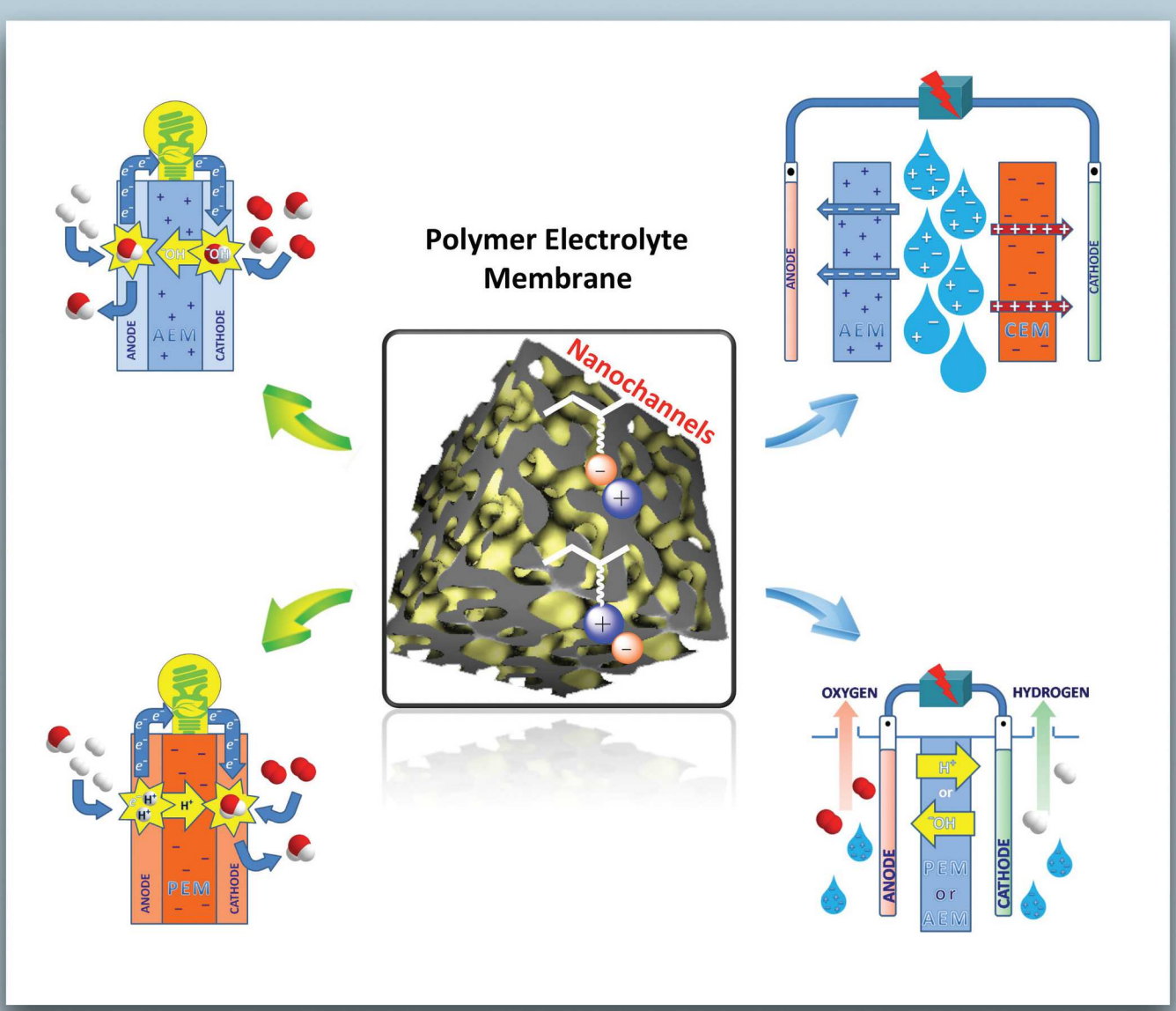

ACS Publications
MOST TRUSTED. MOST CITED. MOST READ.
www.acs.org

Macromolecules

Perspective

pubs.acs.org/Macromolecules

Ion Transport by Nanochannels in Ion-Containing Aromatic Copolymers

Nanwen Li[†,§] and Michael D. Guiver*[,†,‡]

[†]National Research Council, Ottawa, Ontario K1A 0R6, Canada

[§]School of Chemical and Biomolecular Engineering, Georgia Institute of Technology, 311 Ferst Dr. NW, Atlanta, Georgia 30332, United States

[‡]Department of Energy Engineering, College of Engineering, Hanyang University, Seoul 133-791, Republic of Korea

ABSTRACT: The search for the next generation of highly ion-conducting polymer electrolyte membranes has been a subject of intense research because of their potential applications in energy storage and transformation devices, such as fuel cells, vanadium flow batteries, membrane-based artificial photosynthesis, water electrolysis, or water treatment processes such as electrodialysis desalination. Nanochannels that contain ionic groups, through which "hydrated" ions can pass, are believed to be of key importance for efficient ion transport in polymer electrolytes membranes. In this Perspective, we present an overview of the approaches to induce ion-conducting nanochannel formation by self-assembly, using polymer architecture such as block or comb-shaped copolymers. The transport properties of ion-containing aromatic copolymers are examined to obtain an insight into the fundamental behavior of these materials, which are targeted toward applications in fuel cells and other electrochemical devices. Challenges in obtaining well-defined nanochannel morphologies, and possible strategies to improve transport properties in aromatic copolymers having structures with the potential to withstand operation in electrochemical/chemical devices, are discussed. Opportunities for the application of ion-containing aromatic copolymer membranes in fuel cells, vanadium flow batteries, membrane-based artificial photosynthesis, electrolysis, and electrodialysis are also reviewed. Research needs for further improvements in ionic conductivity and durability, and their applications are identified.

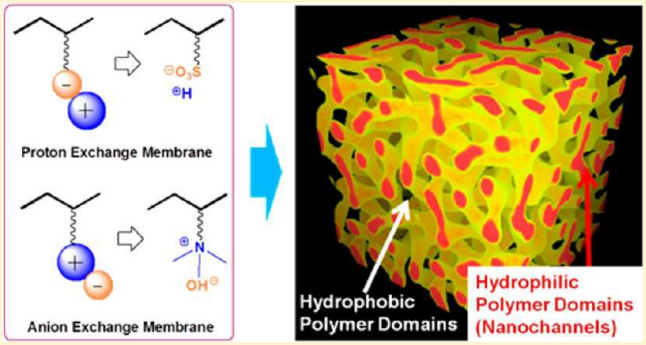

1. INTRODUCTION

The majority of world energy production is derived from the burning of fossil fuels (coal, oil, natural gas, etc.), which results in the emission of large amounts of the greenhouse gas carbon dioxide in addition to environmental pollution from sulfur and nitrogen oxides. Much effort has been expended on the development of membrane-based renewable energy sources and energy storage and transformation devices, such as polymer electrolyte membrane fuel cells,[1−4] redox flow batteries,[5] and hydrogen production for fuel cells (water electrolysis[6−9] and membrane-based artificial photosynthesis[10]). These technologies rely upon ion-containing polymer electrolyte membranes that separate and transport ions between the anode and cathode to balance the flow of electrons in an external circuit.[11] Therefore, they play a central role in determining the efficiency of the devices since ionic transport is a kinetic bottleneck compared with electrical conductivity.[12] These ion-containing polymeric membranes should meet several requirements: reasonable ionic conductivity, good chemical, hydrolytic and dimensional stability, durability in the actual device (electrochemical/chemical) environment, mechanical toughness, adequate heat endurance, and low permeability to gas or liquid.[1,12] Typically, the membranes used in electrochemical devices consist of polymers with fluorinated or hydrocarbon backbones with ion exchange sites[13] (i.e., mostly sulfonic acid[1,12] or quaternary ammonium groups[3,4]) that require water of solvation for effective ion transport to provide adequate device performance. Thus, ion-containing polymeric membranes are broadly divided into proton exchange membranes (PEMs) with fixed negatively charged functional groups such as sulfonic acid and anion exchange membranes (AEMs) with fixed positively charged functional groups such as quaternary ammonium, as shown in Figure 1.

Perfluorosulfonic acid (PFSA) polymers have been commercialized for many years and were originally utilized in the chloralkali industry.[11] Among PSFAs, Nafion (DuPont) is well-known as one of the most promising state-of-the-art PEMs.[1,11] However, these materials have limitations in their utility and performance because of several shortcomings such as reduced proton conductivity at elevated temperatures (>80 °C) due to relatively easy dehydration, high methanol/gas diffusion, poor environmental recyclability and significant manufacturing costs.

Received: October 31, 2013
Revised: February 10, 2014
Published: February 18, 2014

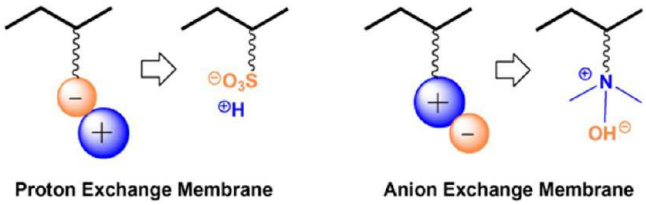

Figure 1. Representation of typical ion-containing polymers for proton exchange membranes (PEMs) and anion exchange membranes (AEMs).

As alternatives, acid-functionalized aromatic hydrocarbon-based PEM copolymers are considered due to their excellent mechanical toughness, film-forming ability, higher glass transition temperatures, and thermal stability.[1,12] However, aromatic PEMs often exhibit inferior ion transport properties at the desired electrochemical operating conditions, such as insufficient proton conductivity at elevated temperatures (>80 °C) and reduced relative humidity (<50%) in hydrogen fuel cells.[2,14]

Counterpoint to PEMs with tethered acidic groups is cationic polymeric AEMs that conduct anions. AEMs provide an environment for electrochemical reactions at high pH that may free electrochemical devices such as fuel cells from platinum catalysts—a current requirement for PEM fuel cells that operate in an acidic environment. AEMs have been long known in water treatment applications such as electrodialysis,[16] but investigations of their potential as solid-state electrolyte membranes for fuel cells and electrolysis are still in their infancy. Several key membrane hurdles must be overcome, namely, improving chemical, dimensional, and mechanical stability and hydroxide conductivity in membranes, to produce high power density devices with long operational lifetimes.[3,4]

Therefore, the control of morphology and thus improvement of ionic transport in both aromatic copolymer-based PEMs[2,14] and AEMs[16,17] have been under intense investigation. In this Perspective, we highlight the morphological development in sulfonated and quaternized aromatic copolymers and observations on their solid-state structures. This review is restricted to the synthesis and properties of well-defined ion-containing aromatic copolymers (i.e., proton and anion exchange) cast into membranes, largely by solution processing techniques. Challenges in obtaining well-defined nanochannels morphology and strategies to obtain durable aromatic copolymer membranes are presented. New opportunities for applications of ion-containing membranes in other electrochemical devices (such as vanadium flow batteries, membrane-based artificial photosynthesis, water electrolysis, and electrodialysis) are also discussed.

2. PROTON EXCHANGE MEMBRANES

It is generally accepted that two types of proton-conducting mechanisms in proton exchange membranes (PEMs) occur: the *vehicle mechanism* and the *Grøtthuss-type mechanism,* also called *structure diffusion.*[18,19] The *vehicle mechanism*, which has been reported to occur in a variety of environments[20] (aqueous acidic solutions,[21] acidic polymers,[22] etc.), occurs by the formation of an ion adduct composed of a proton and a diffusible carrier molecule (e.g., H_2O). The *Grøtthuss-type mechanism* is the transport of protons from site to site without a carrier molecule, and its activation energy depends on the hydrogen bond breaking energy and the distance between sites.[24−26] In most cases, these two proton-conducting mechanisms are not entirely separate from one another and occur simultaneously to some degree. Early studies using pulsed field gradient (PFG) spin echo ^{1}H NMR,[26−29] which is an effective, convenient, and reproducible method to access quantitative data on how water and protons diffuse in PEMs, indicated that the dominant mode of proton conduction in Nafion at low relative humidity (RH) is via the *vehicle mechanism*, while for PEMs in a high humidity environment, protons are rapidly exchanged between hydrated proton exchange sites via the *Grøtthuss mechanism.*[20]

Proton conduction at low RH requires that water diffuses through the membrane, which can occur effectively through continuous hydrophilic pathways by the *vehicle mechanism*, such as those found in Nafion.[18] Thus, current research has focused on the development of alternative aromatic PEM materials which, like Nafion, present nanophase-separated morphology between the hydrophobic polymer main chain and the acidic moieties, leading to conducting nanochannels (ideal morphology for PEMs is shown in Figure 2) responsible for water uptake and proton transport. Atomic force microscopy (AFM), transmission electron microscopy, and small-angle X-ray scattering (SAXS) are usually employed to characterize the presence and morphological structure of nanochannels, although these techniques have distinct limitations. For example, the AFM provides information only on the membrane surface morphology, which is not representative of the bulk morphological structure. Similarly, TEM experiments are usually performed on ∼100 nm films cut by ultramicrotomy. Therefore, the images integrate the morphological structure

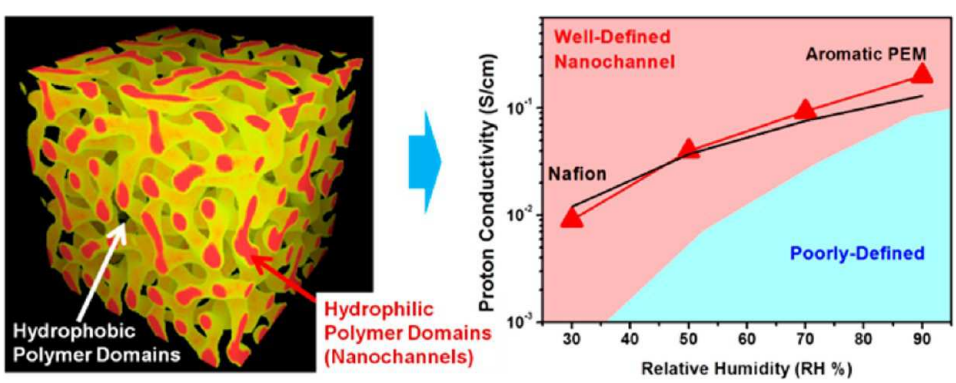

Figure 2. Ideal morphology of PEMs and proton conductivity as a function of relative humidity for aromatic comb-shaped poly(arylene ether sulfone) with well-ordered nanochannels. Reproduced with permission from ref 24. Copyright 2011 Wiley.

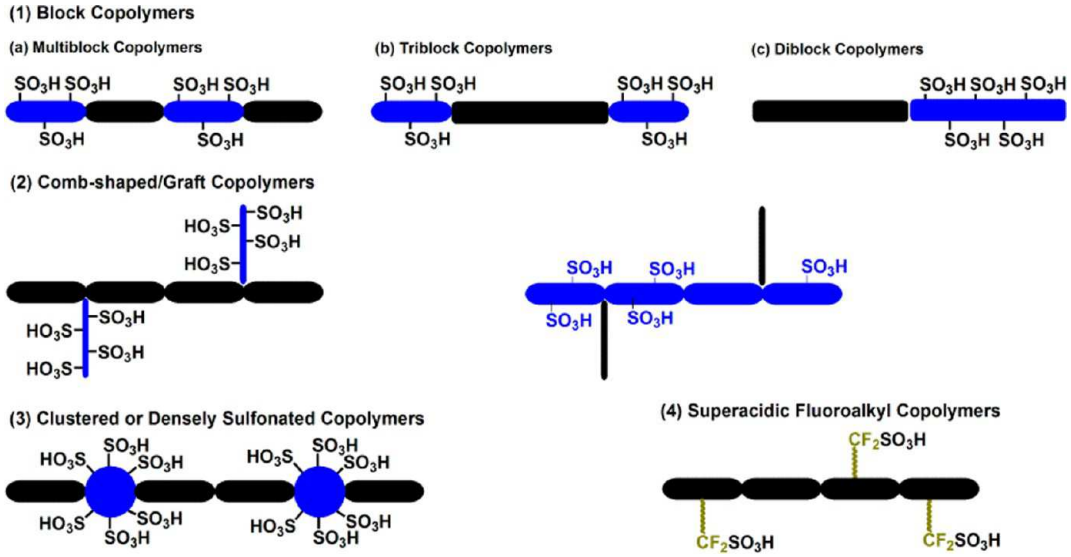

Figure 3. Illustrations of several polymer architectures for PEMs to induce ion-conducting nanochannel formation.

Scheme 1. Polycondensation Methods for Multiblock Copolymers, Limiting Ether–Ether Exchange (End-Capping,[39] Chain Extender,[40,41] Imidization Coupling,[42] and Excess $CaCO_3$ Methods[43])

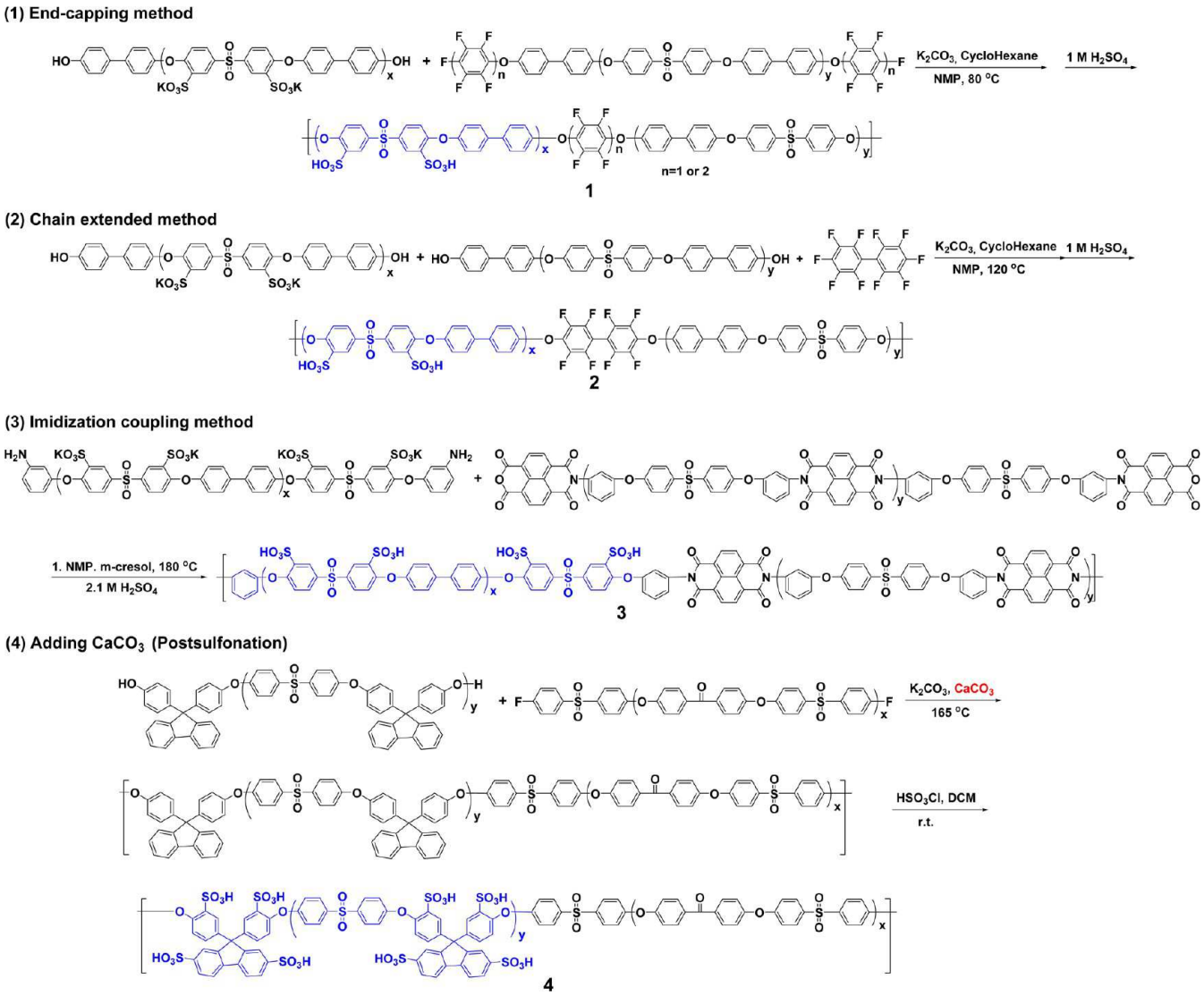

over 100 nm, which implies that overlapping intensity from randomly distributed 1−10 nm diameter channels through the film thickness will significantly distort the spot sizes in the image. Finally, the SAXS gives information averaged over the entire sample. However, the studies have demonstrated significant enhancement in proton conductivity by forming nanochannels and have shown conductivities across a wide range of temperatures and relative humidities that are higher than Nafion. Strategies to obtain well-defined nanochannels by nanophase separation in sulfonated aromatic copolymers have been pursued using multiblock, comb-shaped/graft, clustered, and superacidic fluoroalkyl sulfonated copolymers (Figure 3). Most of these copolymer systems are based on poly(arylene ether)s, polyimides, and polybenzimidazoles. In 2005, Kawakami et al.[30] reported that block copolyimides were more proton conductive than random copolymers for wholly aromatic sulfonated polyimide systems. However, one major obstacle preventing polyimide ionomers from being utilized as PEMs is the inherent hydrolytic instability of imide rings.[31] In the case of sulfonated polybenzimidazoles, sequenced polymers have a higher conductivity than the random ones, but they exhibit very low proton conductivities of $\sim 10^{-4}$ S/cm because of acid−base interactions.[32] Polybenzimidazoles doped with H_3PO_4 acid−base composite membrane are used for high temperature fuel cells, which are operated in the absence of humification.[33] Herein, PEMs based on aromatic poly(arylene ether), which are synthesized by nucleophilic aromatic substitution polycondensation are reviewed predominately.

2.1. Sulfonated Block Copolymers. Block copolymers having low polydispersity have been prepared using controlled/living radical polymerization techniques combined with efficient coupling reactions.[34,35] Their structures provide a template, where phase separation occurs on a nanometer scale due to the thermodynamic incompatibility between unlike blocks. These form a variety of self-assembled morphologies including spheres arranged on a cubic lattice, hexagonally packed cylinders, interpenetrating gyroids, and alternating lamellae.[36] Various kinds of diblock or triblock copolymers with fully or partly sulfonated blocks have been studied as PEMs.[37] Self-organization of these block copolymers offers the opportunity for precise control of membrane morphology by manipulation of chemical compositions and relative volumes of the constituent blocks. Phase-separated morphology can be exploited for the construction of stable proton channels for PEM application, in which hydrophilic sulfonated polymer segments are responsible for the ion-conducting nanochannels, while hydrophobic segments control dimensional swelling in water and enhance the mechanical properties. However, the synthesis of most di- and triblock copolymers relies on styrene and vinyl block systems, which have poor thermal stability and particularly poor chemical and oxidative stability when used in proton exchange membrane fuel cell applications.[37,38]

Multiblock copolymers based on chemically more robust aromatic polymer backbones were developed by relatively few researchers. Generally, the approaches to prepare multiblock copoly(arylene ether)s (e.g., coupling reactions between two different telechelic oligomers via nucleophilic aromatic substitution) are highly limited since their high reaction temperatures (180 °C) can randomize hydrophilic/hydrophobic sequences by well-known ether−ether exchanges, which can take place under nucleophilic step growth copolymerization conditions. Of the various approaches to prevent the ether−ether exchange reactions, lowering the reaction temperature by end-capping[39] and chain extender methods,[40,41] using an imidization coupling reaction[42] and using $CaCO_3$ base,[43] are considered effectual methodologies. Consequently, McGrath and co-workers[39,44] utilized perfluorinated aromatics such as decafluorobiphenyl (DFBP) and hexafluorobenzene (HFB) as the linkage groups between the hydrophilic and hydrophobic oligomers (end-capping method), as shown in Scheme 1-(1). Their highly reactive nature in nucleophilic aromatic substitution reactions permits a significantly lower coupling reaction temperature (80 °C), which minimizes side-reactions, including the ether−ether exchange reaction. The properties of multiblock copolymers **1**[39] have been compared against statistical random sulfonated poly(arylene ether sulfone) (SPAES). Excellent proton conductivity up to 320 mS/cm in water at 80 °C (IEC = 2.29 mequiv/g) was achieved compared with Nafion 117, (σ = 100 mS/cm). In particular, very high proton conductivity has still been observed under low humidity (RH ∼ 40%), which is superior to that of Nafion 117. Tapping mode atomic force microscopy (AFM) images of the membranes revealed better-defined phase separation compared to random copolymers having similar chemical structures, which suggests an explanation for the origin of their higher proton conductivity. They further reported the effect of the block length of multiblock copoly(arylene ether)s on the properties.[45,46] With an increase in block length, the extent of phase separation and the connectivity between the hydrophilic domains increased to form nanochannels. This seems to be the reason for highly effective proton transport. Thus, the membrane with the longest block length (8K:8K) exhibited the highest proton conductivity under low-humidity conditions despite its lowest IEC value (1.28 mequiv/g) in the series, which was comparable to that of Nafion 112. A similar trend is found for the self-diffusion coefficient of water, as determined by PFG NMR.[46] Larger self-diffusion coefficients of water indicate more distinct phase-separated morphology with well-ordered nanochannels. This infers that increasing block length in linear copolymers leads to greater phase separation, as previously visualized from transmission electron microscopy (TEM) images.

The oligomer method as a route to SPAES multiblock copolymers has also been demonstrated by the groups of Kerres,[47] Ueda,[40,41] and Jannasch.[48] In these systems, DFBP was used as a chain extender (Scheme 1-(2)) rather than a monomer. Multiblock SPAES **2** were synthesized by polycondensation of hydrophilic oligomer, hydrophobic bisphenol-terminated oligomer, and the chain extender DFBP.[40,41] These membranes are thus considered as random multiblock copolymers in which hydrophilic and hydrophobic segments are statistically distributed. The TEM and AFM images of the membranes confirmed hydrophilic nanochannel phase-separated morphology. In all cases, the random multiblock copolymers showed considerably higher conductivity (∼2−7 times) than the analogous statistical random SPAES copolymers. However, lower proton conductivity for randomized multiblock copolymers (6.1 mS/cm, 50% RH, 80 °C) than that of the multiblock copolymers (8.6 mS/cm, 50% RH, 80 °C) having similar IEC values (∼2 mequiv/g) was observed.[41]

Another platform for constructing hydrophobic blocks in multiblock copolymer-based PEMs is polyimide because of its excellent thermal stability, high mechanical strength, and good film-forming ability. In order to improve the hydrolytic resistance of imide rings under acidic conditions, the less strained six-membered polyimide ring has been employed by

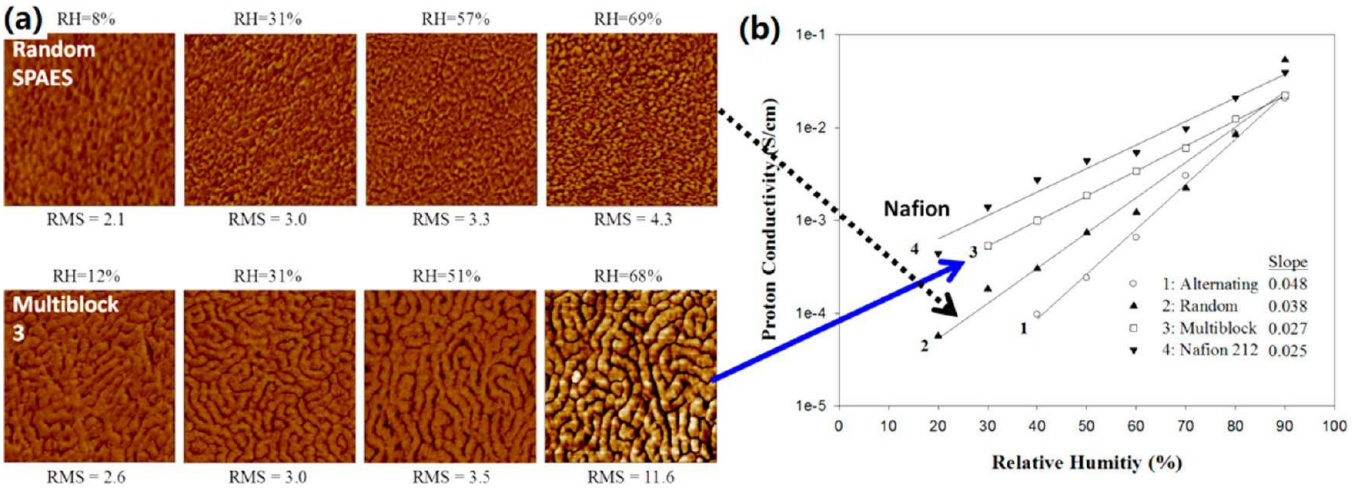

Figure 4. (a) SAFM images of random (top) and multiblock (bottom) PEMs as a function of RH. Image size is 1 μm^2, and phase range is 40° for all images. (b) Conductivity as a function of relative humidity at 80 °C (Nafion is shown for comparison). Reproduced with permission from ref 49.

Scheme 2. Chemical Structures of Highly Sulfonated Poly(phenylene sulfone)-Based Multiblock Copolymers

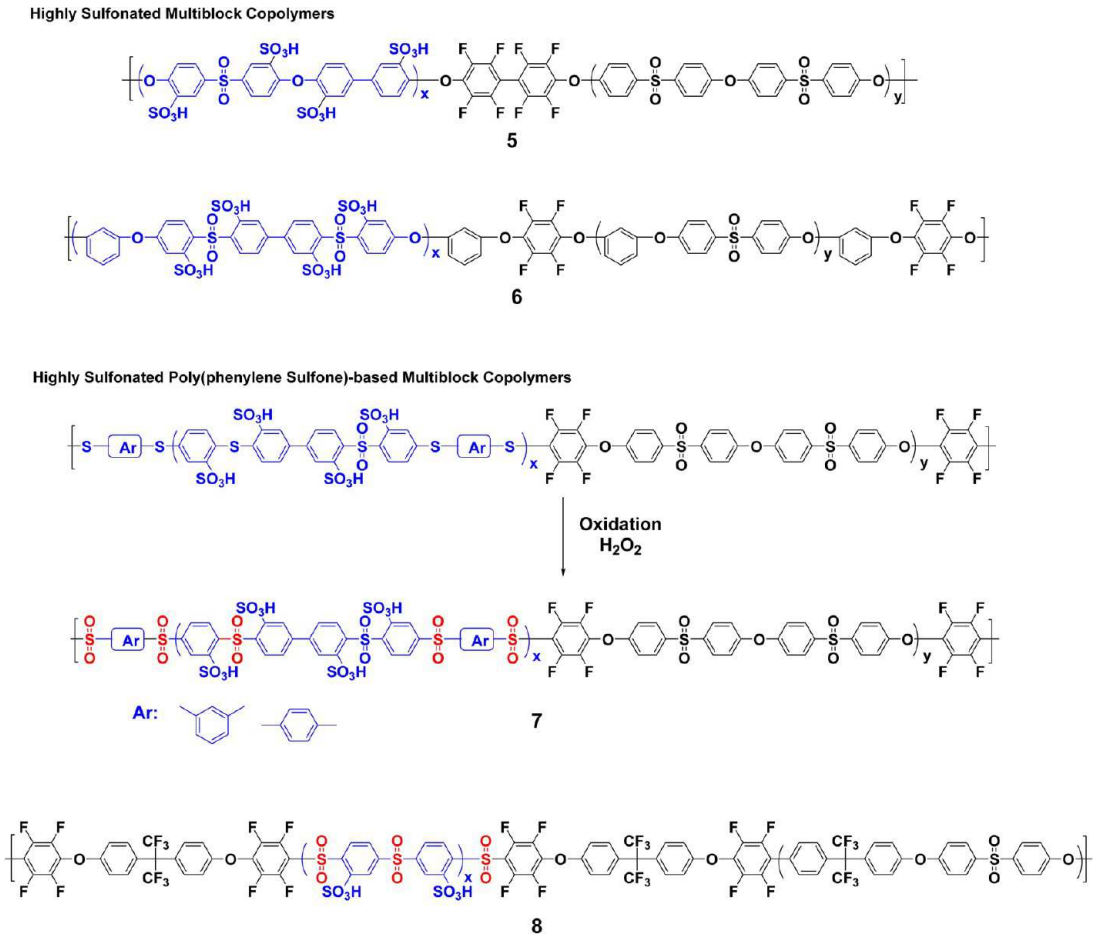

McGrath and co-workers.[42] Amine-terminated sulfonated poly(arylene ether sulfone) hydrophilic blocks were coupled with naphthalene dianhydride-based polyimide hydrophobic blocks via a one-pot imidization, which could reduce the occurrence of ether−ether exchange, as shown in Scheme 1-(3). Scanning atomic force microscopy (SAFM), measured as a function of RH, was used to observe water absorption and swelling of the hydrophilic domains in these multiblock membranes **3**. Compared with the analogous alternating and random copolymers, the multiblock copolymer showed a well-defined "fingerprint image" structure with continuous hydrophilic nanochannels and hydrophobic pathways; the hydrophobic and hydrophilic domain sizes were 57 ± 17 and 23 ± 10 nm, respectively (Figure 4).[49] The conductivity versus RH behavior of the multiblock copolymer had a similar slope compared with Nafion (~0.026). The slope of the multiblock

was lower than that of random copolymer (0.038), meaning that the conductivity of the latter was more dependent on RH than that of Nafion and the multiblock copolymer.

In addition to end-capping, chain extender, and imidization coupling, the use of excess calcium carbonate base catalyst has been another effective method to construct oligomers without reverse polycondensation (ether−ether exchange) or main chain cleavage occurring. Employing this approach, Miyatake et al.[43,50] reported multiblock sulfonated poly(arylene ether sulfone ketone)s **4**, in which the structure of the sulfone−ketone hydrophobic blocks enabled complete sulfonation (Scheme 1-(4)). The high concentration of sulfonic acid groups within the hydrophilic blocks was anticipated to increase the hydrophilicity of these blocks and to result in enhanced phase separation between the hydrophilic and hydrophobic blocks. Thus, rodlike hydrophilic interconnected aggregates were observed to form hydrophilic nanochannels. Small-angle X-ray scattering (SAXS) further confirmed the presence of nanochannels;[43] the distance between the hydrophilic or hydrophobic domains in the hydrated membrane was about 11 nm, which is in agreement with the scanning transmission electron microscopy (STEM) results. These hydrophilic nanochannels induced efficient proton transport in highly sulfonated multiblock copolymers. One particular SPESK membrane (IEC = 1.62 mequiv/g), having 36 sulfonic acid groups in the hydrophilic block, showed higher or similar proton conductivity in comparison to that of Nafion over a wide humidity range at 80 °C. The most important characteristic is that high proton conductivity was retained even at 110 °C.

Much recent work has focused on highly sulfonated multiblock copolymer architecture.[51−55] Ueda and co-workers[51] prepared highly sulfonated multiblock copolymers **5** by combining a chain extender method with postpolymerization sulfonation using concentrated sulfuric acid (Scheme 2). The hydrophilic nanochannels that function as proton transportation channels were observed by AFM. To achieve dimensional stability from high IEC values up to 3.40 mequiv/g, the copolymers were cross-linked using 1,4-diphenoxybenzene in the presence of the condensation agent. The membranes showed 2.4−3.6 times higher proton conductivity compared to Nafion 117 throughout a range of 30−95% RH and still maintained a proton conductivity of 10 mS/cm at 80 °C and 30% RH. These high proton conductivities were believed to originate from efficient proton conduction in the well-defined nanochannels. Jannasch and co-workers developed a tetrasulfonated monomer from which was prepared highly sulfonated multiblock copoly(arylene ether sulfone)s **6** by an end-capping copolycondensation method (Scheme 2).[48] In the monomer, the sulfonic acid groups were introduced exclusively ortho to the sulfone linkages by directed metalation with butyllithium; sulfonic acid groups at these electron-deficient sites are less susceptible to desulfonation. A proton conductivity of 6 mS/cm at 80 °C and 30% RH for **6** membrane with an IEC of 1.83 mequiv/g was achieved, which was compared with 10 mS/cm for NRE 212 under the same conditions. Well-defined hydrophilic nanochannels, which were confirmed by AFM, were believed to be responsible for the high proton conductivity of multiblock copolymers **6**.

To design copolymer structures with further improved chemical stability, Jannasch and co-workers reported poly(phenylene sulfone)-based multiblock copolymers **7** with all of the sulfonic acid groups situated exclusively at the more stable ortho-sulfone site (Scheme 2).[52] Kreuer and co-workers showed that electron-deficient poly(phenylene sulfone)s have excellent hydrolytic and thermooxidative stability due to the absence of electron-donating groups such as ether linkages.[53] Thiol-terminated precursor blocks of sulfonated poly(arylene thioether sulfone) (SPATS)[52] were first prepared via polycondensations incorporating the previous tetrasulfonated monomer. These were coupled with pentafluorophenyl end-capped PAES blocks under mild conditions to form SPATS−PAES block copolymer precursors. The thioether linkages of the SPATS blocks were then selectively oxidized to obtain the SPAS−PAES copolymers containing hydrophilic blocks exclusively with sulfone linkages (Scheme 2). In addition, Meyer and co-workers[54] prepared highly sulfonated blocks by an alternative nucleophilic substitution method involving alkali metal sulfides (Li_2S) and disulfonated monomer. Contrary to the procedure of Jannasch, the highly sulfonated poly(arylene thioether sulfone) block end-capped with pentafluorophenyl was first oxidized by H_2O_2, followed by coupling with phenol-terminated PAES block to form multiblock copolymers **8** (Scheme 2).[54] The novel poly(phenylene sulfone)-based multiblock copolymers **7** and **8** had distinct bicontinuous morphologies with nanochannel sizes of ∼15 nm, as shown by AFM, TEM, or SAXS. Very high proton conductivities were observed, but no hydrolytic and oxidative stabilities and fuel cell durability data were reported. Furthermore, the mechanical properties need to be improved for practical application in fuel cells.[53]

Despite the successful development of numerous multiblock copolymers, the precise control of nanoscale morphology in multiblock copolymers may be limited due to block polydispersity. Diblock or triblock copolymers having low polydispersity have previously been prepared from styrene-type or vinyl monomers using controlled/living radical polymerization techniques combined with efficient coupling reactions.[34−36,56−58] However, the inferior thermal, chemical, and oxidative stabilities and low glass transition temperatures of these types of polymer backbones are less suitable for ion-containing polymers used in applications such as fuel cells.[59,60] To avoid the instability of aliphatic chains, fully aromatic di- or triblock copolymers were designed to improve the chemical and thermal stability and mechanical strength of the PEMs.[61] It is a difficult challenge to design this polymer architecture, since monofunctional terminated aromatic block chains are required to construct di- or triblock copolymers. Although nucleophilic substitution polycondensation reactions are used extensively in making ion-containing aromatic copolymers and they generally provide stable aromatic chains for blocks, they are statistically functionalized with two different reactive groups (e.g., phenol and halogen) at each terminus.

Poly(phenylene oxide)s (PPO) are unique among aromatic polymers in having a monofunctional chain terminus. Different from polycondensation, they are synthesized by catalyzed oxidative coupling of substituted phenol monomers, most usually 2,6-dimethylphenol,[62] resulting in PPOs with single phenoxide-terminated chain ends. 2,6-Diphenylphenol monomer, which polymerizes much more slowly than the commonly used dimethyl analogue (thereby providing a higher degree of control over chain length), provides monophenol-terminated oligomers (often referred to as P3O) in which the pendent phenyl groups are readily sulfonated after combining with a center block by nucleophilic substitution polycondensation, as shown in Scheme 3. The molecular design of this novel class of

Scheme 3. Synthesis of Triblock Aromatic Copolymers 9[61]

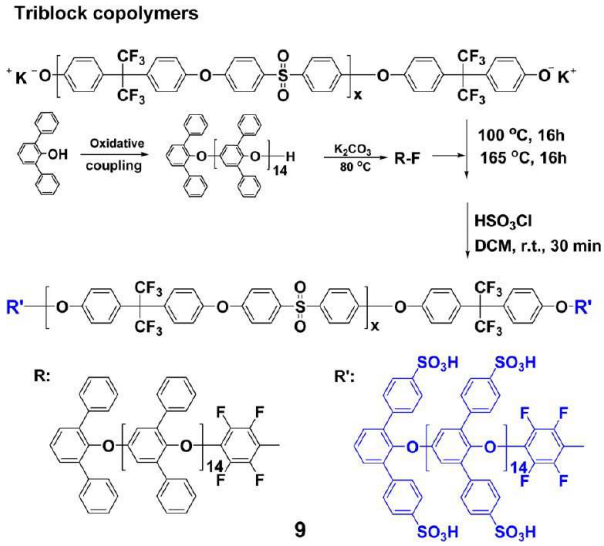

fully aromatic ABA triblock sulfonated copolymers **9**[61] with highly sulfonated P3O A-blocks promoted nanophase separation between the hydrophobic polymer chain and hydrophilic ionic groups. The resulting hydrophilic nanochannels, which were confirmed by AFM and TEM (shown in Figure 5a,b), are responsible for the proton diffusion coefficient and thus proton conduction (Figure 5c). Relative to many other hydrocarbon-based PEMs, the triblock copolymer membranes showed a dramatic enhancement in proton conductivity under partially hydrated conditions (Figure 5d). At 90% RH, which corresponds to the uppermost data point for each membrane sample, the proton diffusion coefficients (D_σ) were higher than that of Nafion 112, even for the lowest IEC triblock membrane (0.97 mequiv/g) having an IEC value similar to Nafion (Figure 5c). The triblock membranes **9** still exhibited relatively good D_σ values of about 2.0×10^{-6} cm^2/s even at 30% RH, which was comparable to that of Nafion 112 (2.67×10^{-6} cm^2/s) and much higher than those of previously reported multiblock copolymer membranes. The results are congruent with the above-mentioned morphological data (well-defined nanochannels) and validate the strategy of fully aromatic triblock copolymers with highly sulfonated blocks having pendent sulfonic acid groups for highly conductive proton exchange membranes.

In addition to nucleophilic aromatic substitution polycondensation, catalyst-transfer polycondensation was also demonstrated to be a promising strategy to synthesize di/multiblock copoly(phenylene)s[63−68] and derivatives with controlled block lengths using a dibromo-/dichlorophenylene derivative having sulfonic acid groups. For example, sulfonated multiblock copolymers polybenzophenone[58] or polyphenylene[68]-*block*-poly(arylene ether)s with high molecular weight and low polydispersity indices were synthesized via Ni-mediated coupling polymerization. The diblock sulfonated polyphenylenes with controlled block length were also synthesized by catalyst-transfer polycondensation of a dibromophenylene derivative having a neopentyl ester protected sulfonic acid group, followed by polycondensation of hydrophobic dibromohexyloxybenzene.[66] Well-developed phase-separated nanochannels were observed in these block copolymers by AFM or TEM, which provided controlled water uptake and sufficiently high proton conductivity, especially at low RH conditions.

2.2. Comb-Shaped or Graft Sulfonated Copolymers. Comb-shaped or graft copolymers are well-known to exhibit distinctly different properties from their linear counterparts of similar compositions. Holdcroft and co-workers demonstrated that graft copolymers displayed better properties, such as lower water swelling and higher through-plane proton conductivity, than those of diblock copolymers via studies of model polymer systems.[69] Thus, various strategies including the copolymerization of oligomers,[70,71] graft-to,[24,72,73] and anionic/atom transfer radical graft-from methodology[74−76] have been reported to achieve specific structural graft or comb-shaped copolymer PEM materials with improved proton conductivity compared to that of conventional polymer architecture.

Among the first reported comb-shaped aromatic copolymers, a highly fluorinated PEM was prepared by copolymerization of aromatic fluorinated monomers with a bisphenol macromonomer containing an oligomeric polystyrene side chain, as shown in Scheme 4.[70] The macromonomer was prepared with controlled molecular weights and low polydispersities by anionic polymerization of α-methylstyrene. Subsequent post-polymerization sulfonation provided tough and flexible comb-shaped PEMs **10**. The investigation showed that a continuous network of ion domains evolves with increasing IEC values as confirmed by TEM, SAXS (Figure 6), and small-angle neutron scattering (SANS).[71] The narrow peak profiles of the first-order peaks in SAXS for copolymers indicate that the ionic domains are uniform. The SAXS profiles of the copolymers also display weak secondary scattering peaks, suggesting a level of longer-range order within the membranes. As a result, the phase-separated nanochannels in the comb-shaped polymers enhance proton conductivity in the high-ionic-content regime. Detailed studies by SANS[71] suggest the comb-shaped copolymer

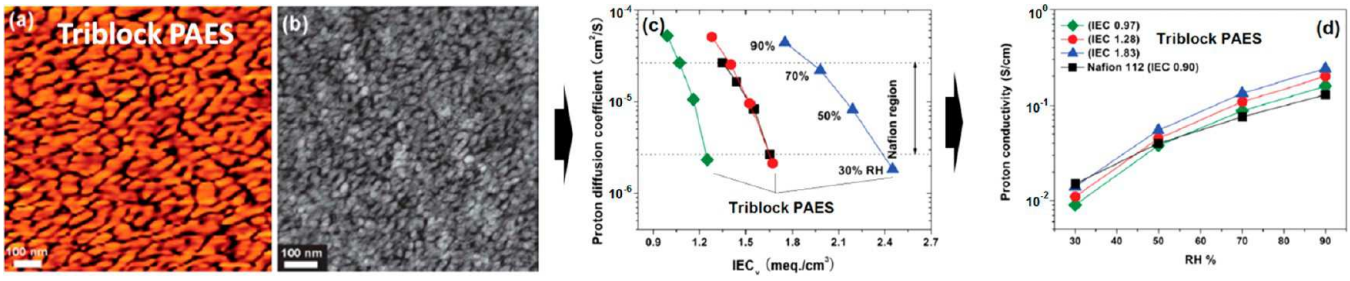

Figure 5. (a) AFM tapping phase image of surface. (b) TEM image of cross-section for **3** (×70) with IEC of 1.28 mequiv/g. (c) Proton diffusion coefficients. (d) Conductivity as a function of RH at 80 °C (Nafion is shown for comparison). Reproduced with permission from ref 51. Copyright 2010 Royal Society of Chemistry.

Scheme 4. Synthesis of Comb-Shaped/Graft Sulfonated Copolymers by Copolymerization with Oligomer,[70] "Graft-from",[74−76] and "Graft-to" Methods[24]

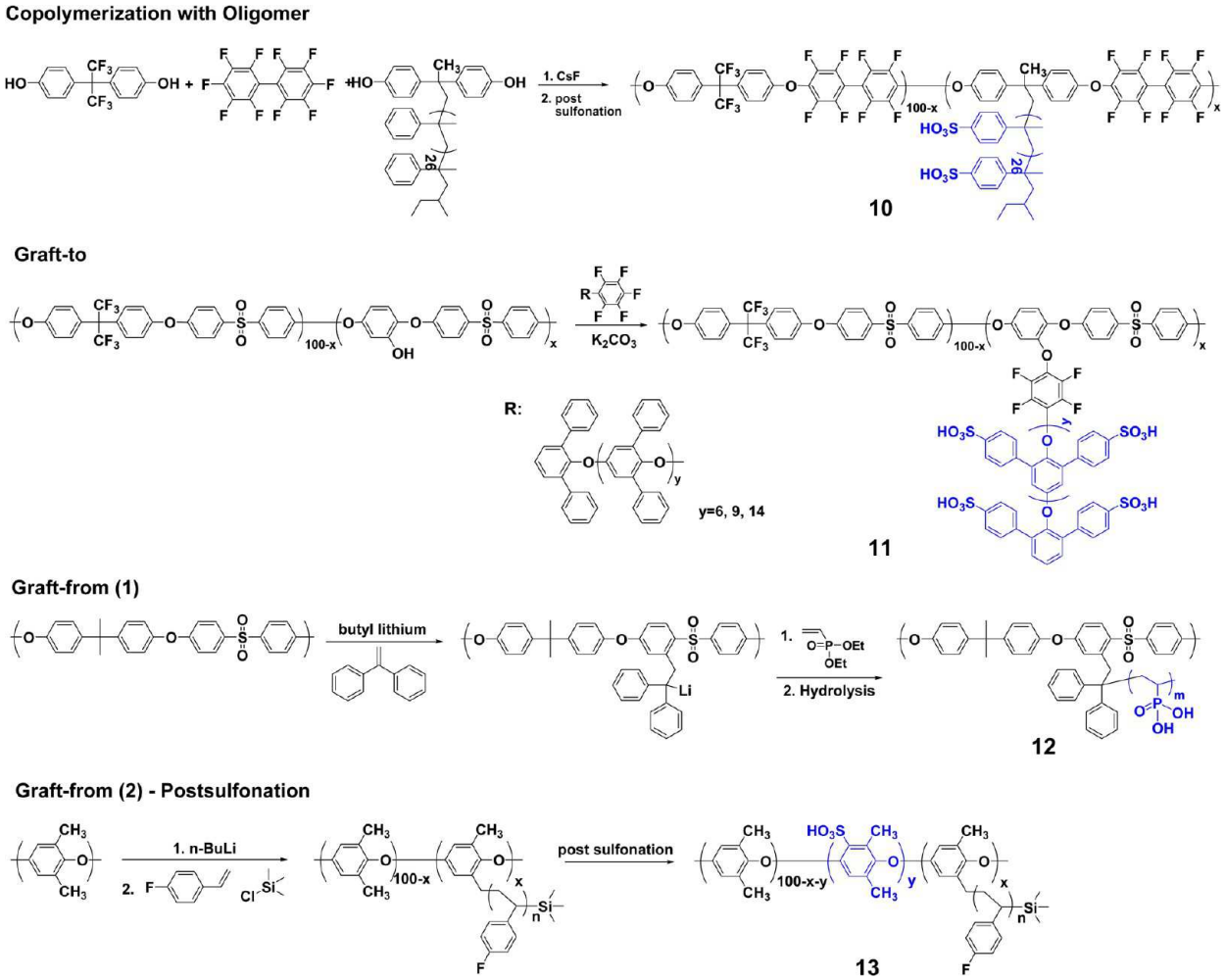

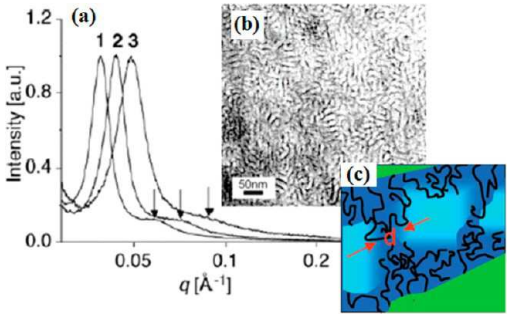

Figure 6. (a) SAXS results of comb-shaped copolymer **10** with different IEC values. (b) TEM images of lead-stained samples **10** with the IEC of 0.87 mequiv/g (the dark regions are (lead-stained) water channels). (c) In the model derived from SANS data, green represents hydrophobic domains (polymer backbone) and the blue represents hydrophilic domains (polymer side chains and water). Adapted with permission from ref 70 (copyright 2006 Wiley-VCH) and from ref 71.

morphology has interconnected ellipsoidal water channels oriented more or less isotropically, within which ionomer aggregates are randomly distributed. Although the initial performance of the comb-shaped copolymer was comparable to or higher than that of the Nafion and another hydrocarbon PEM in the direct methanol fuel cell, the poly(α-methylstyrene) side chain was observed to be highly susceptible to chemical degradation under fuel cell conditions, which caused a loss of the proton conducting sites and performance.[60] The phase separation induced by the structural architecture of comb-shaped copolymers illustrates their potential for achieving good fuel cell performance, but points to the necessity of incorporating chemically more robust designs.

To avoid the relative instability of aliphatic or styrenic chains, fully aromatic comb-shaped copolymers were designed using "graft-to" methodology,[24] to improve the chemical and thermal stability and mechanical strength of the PEMs. This was achieved by combining an OH-functionalized polymer main chain with the monofunctional terminus of the aromatic P3O oligomer. Postpolymerization sulfonation on the pendant phenyl groups with chlorosulfonic acid resulted in the target sulfonated comb-shaped copolymers **11** (Scheme 4)[24] with IECs in the range of ranged from 0.92 to 1.72 mequiv/g. The TEM images show apparently wormlike hydrophilic nanochannels, with little evidence of dead-end channels or larger spheroidal clusters. Analogous to block copolymers, similar IEC values can be derived from comb-shaped copolymer architecture, which permits graft periodicity (X) and graft length (Y) to be altered. The ionic domain size and connectivity are dependent on the IEC value, graft periodicity, and length. In the case of the comb-shaped copolymer with the

lowest IEC (X5-Y6, IEC 0.92 mequiv/g), the morphology has the appearance of a wormlike interconnected hydrophilic network of small ionic clusters 3−5 nm in size, similar to that of Nafion, which has ionic cluster morphology of 5−10 nm in size, interconnected by narrow ionic nanochannels. A comparison of the morphology of two of the copolymers having similar IEC values, one with more periodic but shorter grafts (X5-Y9, IEC 1.28 mequiv/g) and one with less periodic but longer grafts (X3-Y14, IEC 1.26 mequiv/g), suggests that the latter copolymer has the highest interconnectivity in the ionic domains.[24] Paradoxically, the former copolymer has significantly higher proton conductivity, which could possibly be explained by the more periodic shorter graft chains being distributed more homogeneously than the less periodic longer graft counterparts. The interconnectivity of ionic clusters was very pronounced for the copolymer with the highest IEC (X5-Y14, IEC 1.72 mequiv/g), with nanochannel sizes in the range of 15−20 nm. Characteristics of the comb-shaped copolymer **11** membranes were marked anisotropic dimensional swelling, with exceptionally low swelling in the membrane plane direction, but relatively high water uptake in the range of 28−75 wt %, which suggests that the morphology supports high water content without the adverse effects of swelling. High proton conductivities under hydrated conditions (∼100−200 mS/cm, 90 °C, 90% RH) and at reduced humidity (∼10−20 mS/cm, 90 °C, 30% RH) were obtained, which were comparable to, or exceeded that of Nafion 112 (Figure 2).

In addition to the "graft-to" method, Jannasch and co-workers employed anionic graft-from methodology to prepare graft copolymers. As shown in Scheme 4, poly(arylene ether sulfone) (PAES) was grafted with poly(vinylphosphonic acid) (PVPA) by first lithiating PAES with butyllithium,[73,74] capping with 1,1-diphenylethylene to generate 1,1-diphenylalkyl anions, followed by anionic polymerization of diethyl vinylphosphonate (Scheme 4, **12**).[74] The resulting membranes exhibited phase separation because of the inherent immiscibility of the hydrophobic backbone polymer and the strongly hydrophilic grafted chains with very high local concentrations of interacting phosphonic acid (PA) units, giving rise to large hydrogen-bonded nanochannels. These nanochannels enable efficient proton conductivity in the nominally dry state and at a high temperature (120 °C), in spite of the much lower acidity of PA compared with sulfonic acid. For example, at 120 °C, a membrane with a PA content of 57% achieved a conductivity of 4.6 mS/cm under nominally dry conditions and 93 mS/cm under 100% RH, as shown in Figure 7.[74] In addition, Jannasch and co-workers[76] used the anionic grafting-from technique to form graft copolymers with ionic backbones and hydrophobic fluorinated side chains (Scheme 4, **13**). After grafting of the poly(4-fluorostyrene) (PFS) side chains, the PPO backbone was selectively sulfonated under mild and controlled conditions using trimethylsilylchlorosulfonate. Microscopy of solvent-cast membranes revealed copolymer self-assembly into remarkably regular and well-ordered morphologies which, depending on the molecular structure, included lamellar and cylindrical arrangements of the proton conducting ionic nanochannels phase. At a given IEC, the conductivity under fully humidified conditions of all the copolymer membranes exceeded that of a nongrafted sulfonated PPO membrane. The proton conductivity of fully hydrated acidic membranes was above 200 mS/cm at 120 °C.[75]

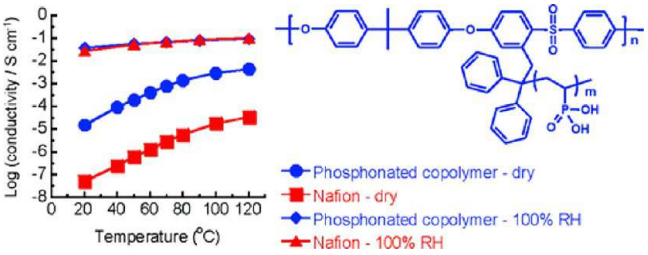

Figure 7. Proton conductivities of graft copolymers **12** and Nafion measured at 100% RH and under nominally dry conditions (the membrane was dried at 40 °C for 1 h under vacuum). Reproduced with permission from ref 74.

2.3. Clustered or Densely Sulfonated Copolymers. In block, comb-shaped, or graft copolymers, the incorporation of hydrophilic and hydrophobic units with highly contrasting polarity into a single polymer chain induces the formation of well-defined phase-separated morphology, which allows effective proton conduction in the resulting nanochannels. Recently, Hay and co-workers[77−80] reported the synthesis of end-functionalized aromatic PEMs with clusters of 6 or 8 sulfonic acid groups at the chain ends. The end group contained clusters of pendent phenyl rings, which are selective sulfonation sites. Soluble and chemically stable wholly aromatic poly(sulfide ketone)s **14**[80] or branched poly(ether ketone)s **15**[78] were prepared, as shown in Scheme 5. Site selective and quantitative sulfonation occurred exclusively at the chain end clusters. The polymers **15** achieved a relatively high proton conductivity (91 mS/cm) with an IEC of 1.05 mequiv/g at 100% RH and 30 °C compared to Nafion (IEC = 0.9 mequiv/g, σ = 94 mS/cm) under the same test conditions. Even at 80% RH, membrane **15** had comparable proton conductivity (29 mS/cm) to that of Nafion (34 mS/cm). Significantly phase-separated, highly interconnected, and wormlike morphologies (nanochannels) with a size of 2−3 nm were observed by TEM.[79] The high ion channel connectivity could be the principal reason for the relatively high conductivities comparable to Nafion, at IEC values similar to Nafion.

The concept of concentrating sulfonic acid moieties into localized clusters has been further demonstrated by the relatively simple and direct introduction of densely sulfonated hydrophilic units into linear polymers.[81−87] Clustered and densely sulfonated units in random copolymers are expected to induce phase separation, which promotes effective proton conduction. For example, random copoly(arylene ether sulfone)s (S4-PAES) **16**[83] and copoly(arylene ether ketone)[84] having localized clusters of four sulfonic acid groups were reported via copolymerization with the sulfonated monomer. Compared to the S2-PAES analogue containing two sulfonic acid groups, the S4-PAES **16** (Scheme 5) membranes displayed lower water uptake and higher proton conductivities, which can be attributed to the more blocky architecture of the clustered sulfonic acid groups in the S4 membranes. Similar to this strategy, Jannasch and co-workers[85] incorporated a tetrasulfonated 4,4′-bis[(4-chlorophenyl)sulfonyl]-1,1′-biphenyl monomer, synthesized by metalation and sulfonation to form densely sulfonated copolymers **17** (Scheme 5).[85] SAXS measurements of the aromatic copolymer membranes with tetrasulfonated units showed ionomer peaks with significantly larger characteristic separation lengths compared with those of the corresponding disulfonated copolymers having similar IEC values. This implies a more efficient phase separation of the ionic groups in the segmented tetrasulfonated copolymer

Scheme 5. Structures of Some Reported Clustered or Densely Sulfonated Copolymers

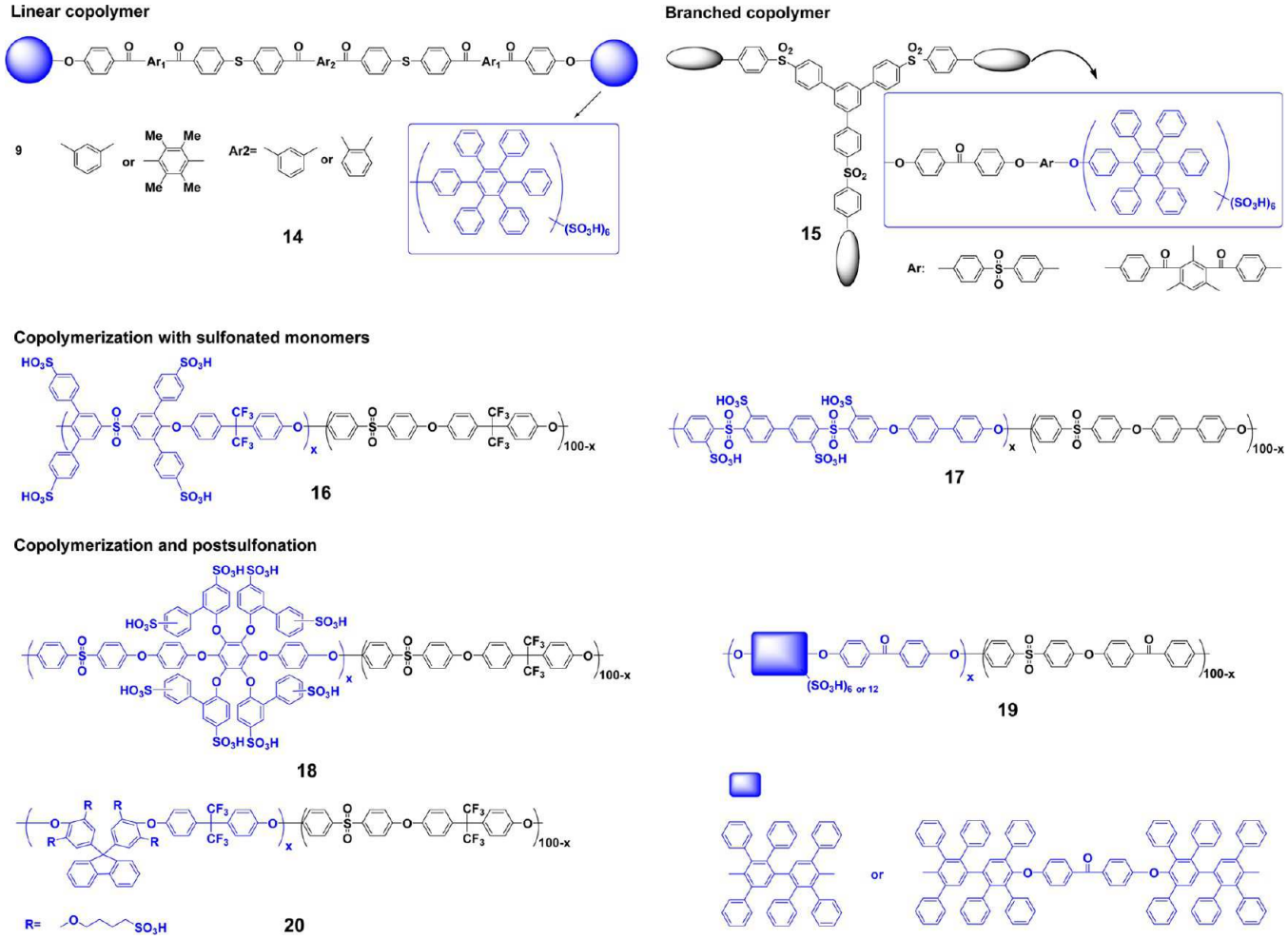

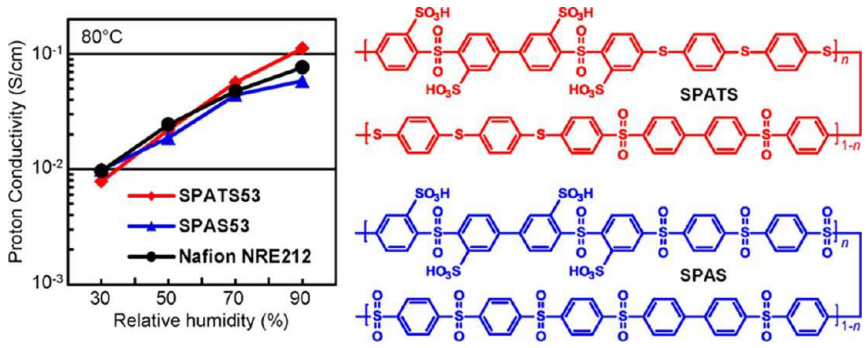

Figure 8. Proton conductivity of the densely sulfonated SPATS53 and SPAS53 membranes under reduced relative humidity at 80 °C. Reproduced with permission from ref 86.

membranes **17**. At reduced RH, the tetrasulfonated copolymer membranes had significantly higher conductivity than the disulfonated ones. As discussed before, to improve the hydrolytic and oxidative stability of the polymer backbone, highly sulfonated poly(phenylene sulfone)s[86] were prepared from tetrasulfonated monomers. Because of the distinct phase-separated morphology induced by the densely sulfonated structures, the SPATS (IEC 2.4 mequiv/g) and SPAS (IEC 2.2 mequiv/g) membranes maintained high proton conductivity at low RH. At 80 °C and 30% RH, the membrane conductivities were 8 and 10 mS/cm, respectively (Figure 8). The latter value coincided with that recorded for the state-of-the-art NRE 212 membrane under the same conditions.

Random copolymers with higher densities or clusters of sulfonic acid groups **18**[81] and **19**[82] with 6, 8, 10, and 12 sulfonic acid groups were synthesized by polycondensation and subsequent postpolymerization sulfonation using chlorosulfonic acid or concentrated sulfonic acid, which occurred exclusively on electron-rich aromatic rings. There was an absence of sulfonation in the electron-deficient phenylene units of the hydrophobic part due to the deactivation by electron-withdrawing sulfone, hexafluoroisopropylidene, or ketone

linkages, as shown in Scheme 5. The IEC was adjusted by varying the monomer ratios. Tapping mode phase images of membranes having 8 and 10 sulfonic acid groups exhibited well-defined phase-separated structures.[81] The hydrophilic domains of the membrane having 10 sulfonic acid groups appeared to be wider and more interconnected than those of membrane with 8 sulfonic acid groups.[87] The proton conductivity of the membrane having 10 sulfonic acid groups (4 mS/cm) was comparable to that of Nafion 117 (3.9 mS/cm) at 30% RH and 80 °C, which was attributed to the more connected proton transport nanochannels, enabling effective migration of hydronium ions.[87]

Guiver and co-workers[88,89] prepared clustered fluorene-based sulfonated poly(arylene ether sulfone) copolymers, one with four flexible pendent butylsulfonic acid units per repeat unit **20** (Scheme 5)[88] and an analogous fluorene-based copolymer with four rigid sulfophenyl groups,[89] using postfunctionalization. In comparison with other representative SPAES structures and with Nafion membranes, the **20** membranes exhibited very low water uptake and dimensional change, even at elevated temperatures (80 °C). The SPAES **20** (IEC = 1.86 mequiv/g) membranes displayed good proton conductivity, which was comparable to or higher than that of Nafion at >50% RH. It appears that the flexible pendent sulfonic acid clusters of both SPAES-33 and SPAES-39 induce interconnected narrow ionic nanochannels (2−5 nm), as shown by TEM, are responsible for the high proton conductivities and low dimensional swelling. In contrast, the analogous membrane in which the cluster of sulfonic acid groups were rigidly tethered onto the bulky fluorene moiety displayed distinct isolated ionic domains that were not interconnected.[89]

To date, most sulfonated multiblock ion exchange copolymers have been constructed by aromatic nucleophilic substitution from monomers in which the ionic group (e.g., sulfonic acid) is on either the nucleophilic or the electron deficient monomer. This gives rise to "gaps" in the ion-conducting groups along the chain. It is well-known that pendent phenyl groups are readily sulfonated on polymers[90] and that the resulting sulfophenylated polymers are oxidatively more stable than those sulfonated on the main chain.[91] By using methodology of placing pendent phenyl groups on both the nucleophilic and the electron-deficient monomers, the latent hydrophilic segment can be postsulfonated after copolymerization so that the sulfonic acids are in closer proximity. Thus, sulfonated segmented copoly(arylene ether sulfone)s were synthesized to increase the proximity of sulfonic acid groups in the conducting segment, which were controlled to 15, 30, and 60 (i.e., X = 5, 10, and 20, respectively). As shown in Figures 9,[92] the phase surface images exhibit clear hydrophilic/hydrophobic phase separation with an interconnected hydrophilic network of small ionic clusters, which is the result of the segmented structure in combination with the densely populated sulfophenylated groups. The interconnectivity of ionic clusters appeared to be more pronounced for the longer hydrophilic block membranes with 60 sequential sulfonic acid groups (X20Y30), which exhibited hydrophilic domains (Figures 9c). Another membrane with 60 sequential sulfonic acid groups (X20Y20) with an IEC value of 1.82 mequiv/g had a proton conductivity of 36 mS/cm at 80 °C and 50% RH, which is comparable to that of Nafion (40 mS/cm). Longer hydrophilic block lengths (more sequential sulfonic acid groups) appeared to be effective in increasing proton diffusion coefficients, which correlated with the proton conductivity

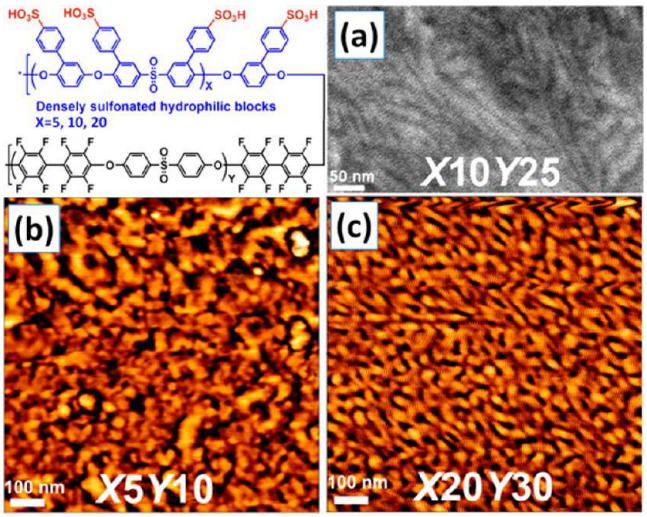

Figure 9. Chemical structure of segmented densely sulfonated copolymers: (a) TEM and (b, c) AFM images. Reproduced with permission from ref 92.

observations. These results demonstrated that the strategy of designing copolymer architecture having densely populated sulfonic acid groups is a promising way to achieve effective proton conducting nanochannels and thus high-performance PEM materials.

2.4. Superacidic Fluoroalkyl Sulfonated Copolymers. PFSA ionomers such as Nafion all have similar structures of highly hydrophobic backbones with flexible superacidic perfluoroalkylsulfonic acid side-chains. One promising approach is to introduce perfluoroalkyl sulfonic acid (superacid) groups into aromatic polymer backbones to induce phase-separated morphology. Compared with the acidity of aryl or alkylsulfonic acid groups ($pK_a \sim -1$), perfluoroalkylsulfonic acids are considerably stronger with pK_a value of ∼−6 and thus tend to be better proton conductors because they can be easy deprotonated under conditions of lower RH.[93−95] Moreover, the large polarity differences between the superacid hydrophilic phase and the fluorocarbon hydrophobic phase induces strong phase separation, forming ionic nanochannels that allow high proton conductivity in a reduced humidity environment. Generally, Cu-catalyzed Ullmann coupling[96−101] and dehalogenation coupling[102] were employed to synthesize superacidic fluoroalkyl sulfonated copolymers, as shown in Scheme 6.

From hydrolysis of commercially available 1,1,2,2-tetrafluoro-2-(1,1,2,2-tetrafluoro-2-iodoethoxy) ethanesulfonyl fluoride, Yoshimura et al.[96] reported poly(arylene ether sulfone)s with $-CF_2CF_2OCF_2CF_2SO_3H$ side chains (**21**, PAES−PSA, Scheme 6), which were synthesized by Cu-catalyzed debromination Ullmann coupling of PAES-Br_2 and potassium 1,1,2,2-tetrafluoro-2-(1,1,2,2-tetrafluoro-2-iodoethoxy) ethanesulfonate (PSA-K). Their initial attempts to cross-couple the PSA-K and polymer were unsuccessful: Methodologies of Williamson ether synthesis using a polymer having a hydroxyl group and PSA-K using potassium carbonate, a nucleophilic reaction using lithiated polysulfone and PSA-K, as well as a Friedel−Crafts reaction using PAES and PSA-K in the presence of $AlCl_3$ all did not proceed or gave only undesired byproducts.[96] Subsequently, Ullmann coupling was used successfully to prepare aromatic PEMs containing perfluorosulfonic acid groups grafted onto various poly(aryl ether) backbones. For example, PEMs based on fluorenyl containing poly(aryl ether sulfone),

Scheme 6. Chemical Structures of Some Reported Superacidic Fluoroalkyl Sulfonated Copolymers

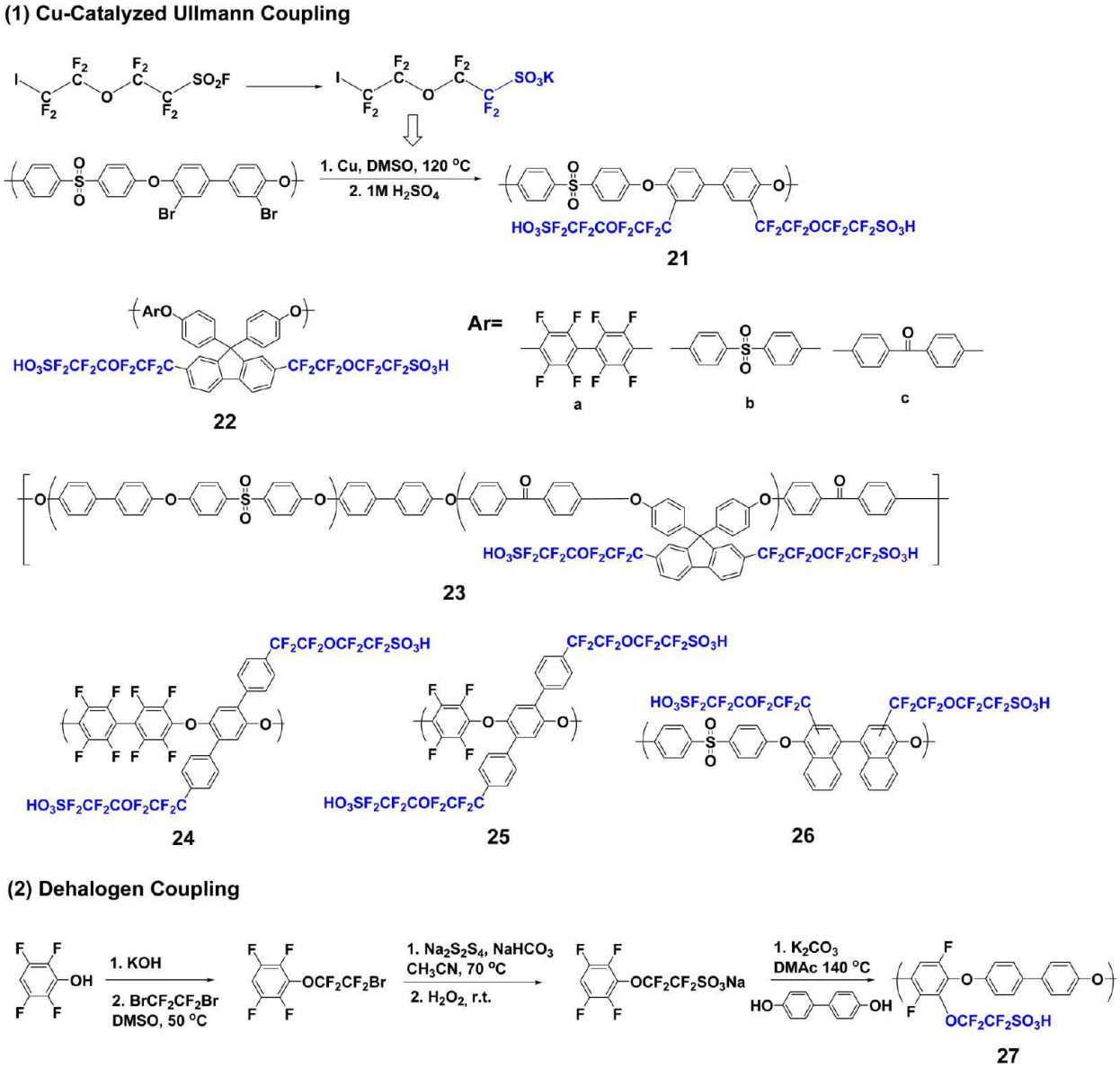

poly(ether ketone) and poly(aryl ether) (**22**, Scheme 6) were reported by Miyatake and co-workers.[97,98] Although the overlapping intensity from randomly distributed 1−10 nm diameter channels in the membrane through the thin film thickness will significantly distort the spot sizes in the TEM image, the perfluorinated superacid groups appear to be more likely to aggregate than the aromatic sulfonic acid groups. Small ionic clusters (dark areas ca. 2−3 nm in diameter) were distributed homogeneously and interconnected throughout the field of view, which formed hydrophilic nanochannels, as shown in Figure 10a. Compared to the PEM having the sulfonic acid groups directly attached to the aromatic rings, the morphology of **22** was more similar to that of Nafion, in which the ionic clusters were ca. 5−6 nm in diameter (Figure 10b). The **22** membranes exhibited substantially higher water uptake than that of SPE with similar IEC values, which was believed to be due to the ordered and interconnected ionic clusters. The membranes showed a large improvement in proton conductivity over the range of 20−90% RH, which was 3−60 times higher than that of corresponding sulfonated aromatic

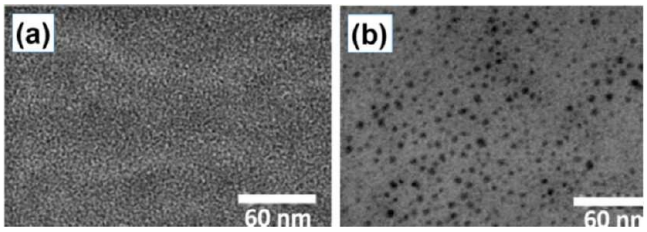

Figure 10. STEM images of (a) **22** (1.52 mequiv/g) and (b) sulfonated polysulfone with aryl sulfonic acid groups (1.59 mequiv/g). Reproduced with permission from ref 98.

polymers. Using similarly structured multiblock fluoroalkyl sulfonated copolymers (**23**, Scheme 6),[99] the resulting membranes exhibited characteristic hydrophilic/hydrophobic phase separation with hydrophilic clusters having dimensions of ∼10 nm, which led to high proton conductivity from relatively low IEC values.

Membranes with higher proton conductivities, achieved by increasing IEC values (>1.50 mequiv/g), maintained dimen-

sional stability in water, although the conductivity was not as high as PFSAs. Ueda and co-workers prepared highly fluorinated **24**, **25**[100] or binaphthyl containing **26**[101] poly(aryl ether)s with pendant perfluoroalkyl sulfonic acid groups (IEC ~ 1.80 mequiv/g) to enhance water resistance of the resulting polymers (Scheme 6). The **25** membrane had high λ values comparable to Nafion 117 (0.90 mequiv/g) regardless of the high IEC value (1.83 mequiv/g). However, the proton conductivity of the **25** membrane with the highest IEC value was higher than that of the Nafion 117 at 80 and 50% RH and comparable to the Nafion 117 membrane even at 30% RH, as shown in Figure 11. AFM images showed well-dispersed and

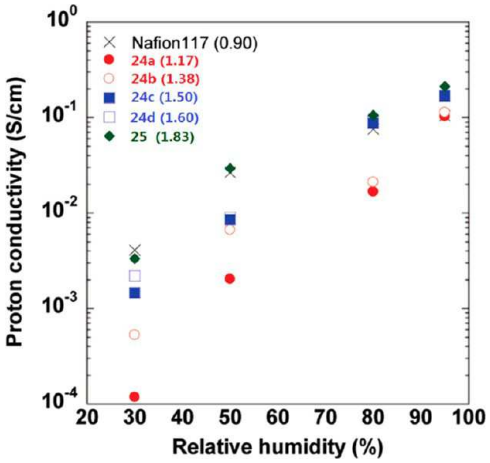

Figure 11. Humidity dependence of proton conductivity of **24**, **25**, and Nafion 117 membranes at 80 °C. Adapted with permission from ref 100.

interconnected hydrophilic domains, which contributes to the formation of proton transport nanochannels and high λ values, resulting in high proton conductivity throughout a wide range of RH.

Apart from Ullmann coupling, another synthetic approach using dehalogenation coupling was reported by Wang and co-workers[102] to prepare a fluorinated aromatic poly(arylene ether) **27** with pendent perfluoroalkyl sulfonic acid groups, as shown in Scheme 6. High proton diffusion coefficients were observed due to the hydrophilic nanochannels, as confirmed by TEM images. The PEMs had conductivities comparable (<50% RH) or superior (>50% RH) to Nafion 115 at 80 °C and at even higher temperatures of 120 °C. Although the polystyrene backbone was chosen, the novel coupling methodology using iridium-catalyzed aromatic C−H activation/borylation and subsequent Suzuki−Miyaura coupling with sulfonated fluoroalkyl bromides could have synthetic utility for the preparation of superacidic fluoroalkyl sulfonated aromatic copolymers.[103]

2.5. Other Strategies. Apart from the synthetic methods mentioned above, other strategies including chemical and physical processing were developing to induce proton transport nanochannel formation in aromatic PEMs. For example, PEMs with very high IEC or subjected to thermal annealing have been reported recently. Physical processing by thermal annealing of a sulfonated multiblock poly(arylene sulfide sulfone nitrile)[104] PEM induced the formation of cocontinuous lamellar morphologies with a nanochannel size of up to 40 nm, as observed by TEM. Another approach is PEMs with high IEC; increasing the IEC is an effective way to increase the conductivity at low RH because it increases the charge carrier concentration and the diffusion coefficient of water, greatly influencing the ionic mobility. Recently, very high IEC (3−8 mequiv/g) PEMs based on sulfonated poly(phenylene sulfone),[53,105] polyphenylene,[63,64] and poly(arylene ether sulfone)[106,107] were reported, which exhibited proton transport nanochannels. However, they tend to be extremely brittle in the dry state and are either soluble or swell excessively in water. Cross-linking has been employed to prevent water solubility and inhibit dimensional swelling. The proton conductivities of cross-linked polyphenylenes with IEC values of ~8 mequiv/g at 80 °C were 4−5 times that of Nafion NR-212 over the whole relative humidity range (20−100 RH %).[64]

In conclusion, many strategies including chemical and physical have been developed to improve the proton transport by forming nanochannels in aromatic PEMs. As shown in Figure 12, aromatic PEMs based on multiblock, comb-shaped,

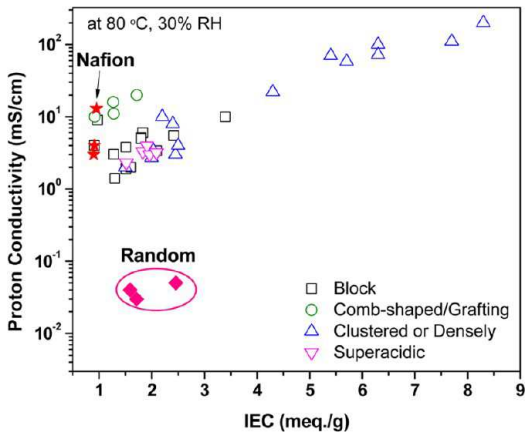

Figure 12. Performance comparison of various types of PEMs: relationship between IEC and proton conductivity at 80 °C, 30% RH.

clustered, or superacidic structures induce nanochannel formation, which results in much higher proton conductivities than those of random PEMs at 80 °C and 30% RH. PEMs with very high IEC values (>4 mequiv/g) had almost 2−10 times higher proton conductivities than that of Nafion membranes. These results demonstrate that the presence of conducting nanochannels facilitates effective proton transport in PEMs. Although some membranes with a low IEC value (~0.9 mequiv/g) had proton conductivity similar to that of Nafion (5−10 mS/cm, at 80 °C and 30% RH), most aromatic PEMs require higher IEC values to achieve similar proton conductivity. Thus, evaluation of water/proton transport behavior needs further exploration through systematic studies. Water diffusion using PFG-NMR and proton conductivity measurements have been utilized to provide complementary information to help understand the membrane transport processes and probe material performance in perfluorosulfonate ionomers.[25−29] Madsen and co-workers[28] reported that the water diffusion anisotropy linearly depends on the degree of membrane alignment (orientational order parameter) which indicates that local hydrophilic channel structure, as well as domain sizes and defect structure (channel connectivity), do not depend on macroscopic deformation. Employing PFG-NMR techniques, McGrath and co-workers[46] found that the block copolymers exhibit larger water self-diffusion coefficients than those of random copolymers, suggesting more distinct phase-separated morphology with well-ordered nanochannels in block copolymers. Recently, the influence of ordered

Scheme 7. Synthesis of Multiblock Quaternized Copolymers 28[116] and 29[16] by Post-chloromethylation and Copolymerization with Chloromethylated Monomer

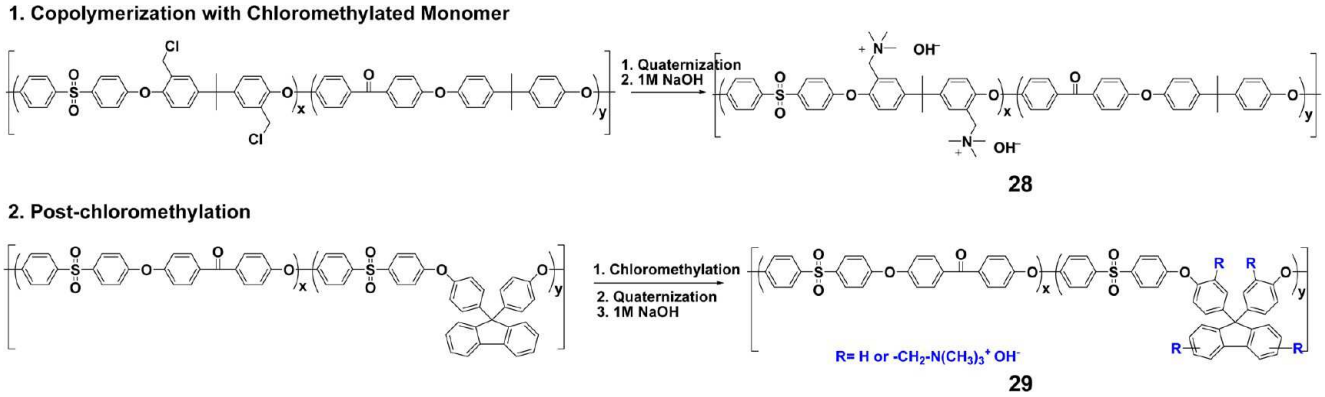

morphology on the transport properties of block copolymers was further investigated by Madsen and co-workers[27−29] using PFG-NMR to measure water diffusion coefficients in the in-plane and through-plane direction. Various levels of water diffusion anisotropy were observed in the multiblock copolymers, where water diffusion in-plane was faster than through-plane. As block mass increases, diffusion anisotropy exhibits an increasing dependence on water uptake, which corroborated the existence of macroscopically aligned lamellae parallel to the membrane plane. However, further studies are needed to understand water and proton transport in aromatic PEMs.

For practical application in fuel cells, the optimum membranes must be morphologically and mechanically stable because the PEMs experience an external uniaxial pressure in the range 2−5 MPa within the fuel cell stacks. In addition, fluctuations in the internal swelling pressure in space and time lead to additional strain. Thus, the mechanical properties of membranes are not only controlled by their storage modulus but also by their elongation to break. Most hydrocarbon membranes have a significantly higher storage modulus than PFSA membranes, but a smaller elongation to break (especially at low hydration levels); i.e., the membranes tend to be more brittle. Thus, cracks and pinholes form more frequently for aromatic PEMs under fuel cell operating conditions. In addition, the chemical degradation, initiated by reactive intermediates such as hydroxyl radicals ($HO^{\bullet}$) present in the membrane, further decreases mechanical properties by chain cleavage. Thus, important targets for future membrane developments should be increased chemical stability and fracture toughness over a large RH range.

3. ANION EXCHANGE MEMBRANES

Generally, lower ionic conductivity in anion exchange membranes (AEMs) is often observed when compared to acidic proton exchange membranes (PEMs) due to the inherently lower mobility of hydroxyl ions and the weak basicity of the cation site.[108,109] For instance, the ion mobility of H^+ is 36.23×10^{-8} $m^2/(s\ V)$, whereas the OH^- is only 20.64 $\times 10^{-8}$ $m^2/(s\ V)$ in the limiting case of an infinitely dilute solution at 298 K.[108,110] Moreover, sulfonic acids are considered as strong acids in PEMs (the pK_a of aryl sulfonic acid has been estimated to be on the order of −1),[110] while quaternary ammoniums are comparatively weak bases with a pK_b on the order of 4. Therefore, dissociation of the quaternary ammonium ions presents a considerable theoretical barrier for efficient hydroxide conduction in an AEM. Hydroxide transport mechanisms could be analogous to that of the transport of protons in PEMs, i.e., the *vehicle mechanism* and the *Grøtthuss-type mechanism* although a *Grøtthuss-type mechanism* is considered to be the dominant transport mechanism based on the fact that hydroxide exhibits *Grøtthuss* behavior in aqueous solutions, comparable to protons.[111−114] However, there are fundamental differences between PEM and AEM conductivities, in spite of the mass diffusion coefficients of hydroxides and protons being similar[115] and the same dominant transport mechanisms through the membrane. Several researchers[111,115] have proposed that the hydronium ions are naturally integrated into the hydrogen-bonding network of water, whereas hydroxide ions tend to have stable solvation shells that reorganize the solvent molecules and perturb the hydrogen bond network. High hydroxide conductivity could usually be achieved only by high ionic content and water uptake, which generally results in significant dimensional swelling in water and loss of the mechanical properties. To date, only a few anion-conductive, nanophase-separated aromatic copolymers have been reported.[16,116−118]

In the pursuit of aromatic PEMs, multiblock copolymers have been shown to be effective in inducing phase-separated morphology with interconnected proton transporting pathways (nanochannels). Utilizing sequential hydrophilic/hydrophobic structures with quaternary ammonium or other positively charged groups in the hydrophilic blocks is also a viable strategy for aromatic AEMs. Zhang and co-workers[117] synthesized quaternized multiblock poly(arylene ether sulfone)s (PAES) by block copolycondensation, followed by bromination using *N*-bromosuccinimide (NBS) as bromination reagent, and then amination. Multiblock copolymers **28**[116] were also synthesized via polycondensation of chloromethylated bisphenol monomer, followed by amination (Scheme 7), to avoid the use of chloromethyl methyl ether, which is carcinogenic and hazardous. By comparing the conductivities of random, sequenced and multiblock copolymer membranes all having similar IEC values, it was found that the multiblock copolymer membrane displayed the highest anion conductivity. High hydroxide ion conductivities up to 56−85 mS/cm at temperatures 30−70 °C were obtained, although no morphological structures were observed. Watanabe and co-workers[16] prepared anion conductive aromatic multiblock copoly(arylene ether)s (QPE, **29**, Scheme 7) with clustered ionic groups in the hydrophilic blocks via block copolycondensation of fluorene-containing oligomers, chloromethylation, and quaternization reactions. As confirmed

by scanning transmission electron microscopic (STEM) (Figure 13), the multiblock structure was responsible for the hydrophobic/hydrophilic phase separation and interconnected ion transport pathway. Consequently, much higher hydroxide conductivities were observed for multiblock copolymer membranes than that of random copolymer membranes, as shown in Figure 12. Thus, the concept of utilizing multiblock copolymer structures with well-defined phase-separated nanochannels appear to be effective for improving the ionic conductivity of AEMs without sacrificing other essential properties such as mechanical and dimensional stability.

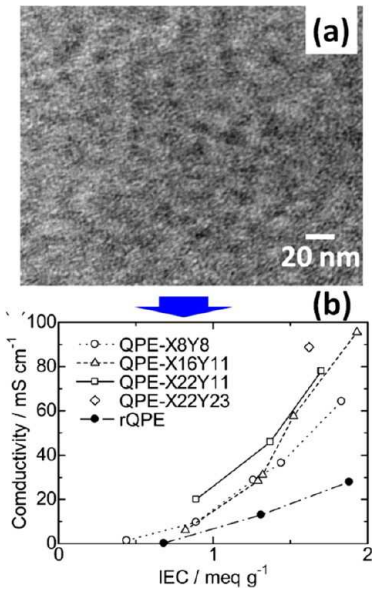

Figure 13. (a) STEM image of **29** membrane (IEC = 0.89 mequiv/g) stained with tungstate ions. (b) Hydroxide ion conductivity at 40 °C of **29** membranes as a function of IEC. Adapted with permission from ref 16.

Apart from multiblock copolymers, comb-shaped architecture[17,119−121] was shown to be another effective strategy for the improvement of hydroxide ion transport, analogous with PEMs. Li et al.[17,119] prepared highly stable comb-shaped anion exchange membranes with improved anionic conductivities. As shown in Figure 14a, comb-shaped poly(2,6-dimethyl-1,4-phenylene oxide)s (PPO) with quaternary ammonium (QA) groups **30** and long alkyl side chains have been synthesized by bromination and amination reaction from inexpensive starting materials.[17,119] The unique polymer architecture results in nanophase separation between the conducting (quaternized PPO) and nonconducting domains (grafted alkyl chains) as confirmed by small-angle X-ray scattering (SAXS) (Figure 14c)[119] and thus gives rise to high anion conductivities. An important characteristic is that the comb-shaped membranes exhibited a much lower water uptake (10−20 wt %) but a comparable conductivity compared with the values reported for many QA-AEMs in the hydroxide form. The high hydroxide conductivity achieved with low water uptake was attributed to well-defined nanophase-separated morphology. Another AEM with pendent QA groups prepared by reaction of Michler's ketone with lithiated polysulfone had similar characteristics of high conductivity and low water uptake, although no morphology was reported.[122] Zhuang and co-workers[120] prepared polysulfones with grafted hydrophobic side chains and QA groups **31** (Figure 14b) to induce the aggregation of hydrophilic domains to form larger and more efficient interconnected ionic channels, such that the local ion concentration increased and the hopping conduction of OH^- was effectively enhanced. This strategy of self-aggregation dramatically boosted the ionic conductivity of AEMs up to 100 mS/cm at 80 °C. Molecular dynamics (MD) calculations confirmed that the OH^- containing water clusters are intercalated in the hydrophobic network formed by the

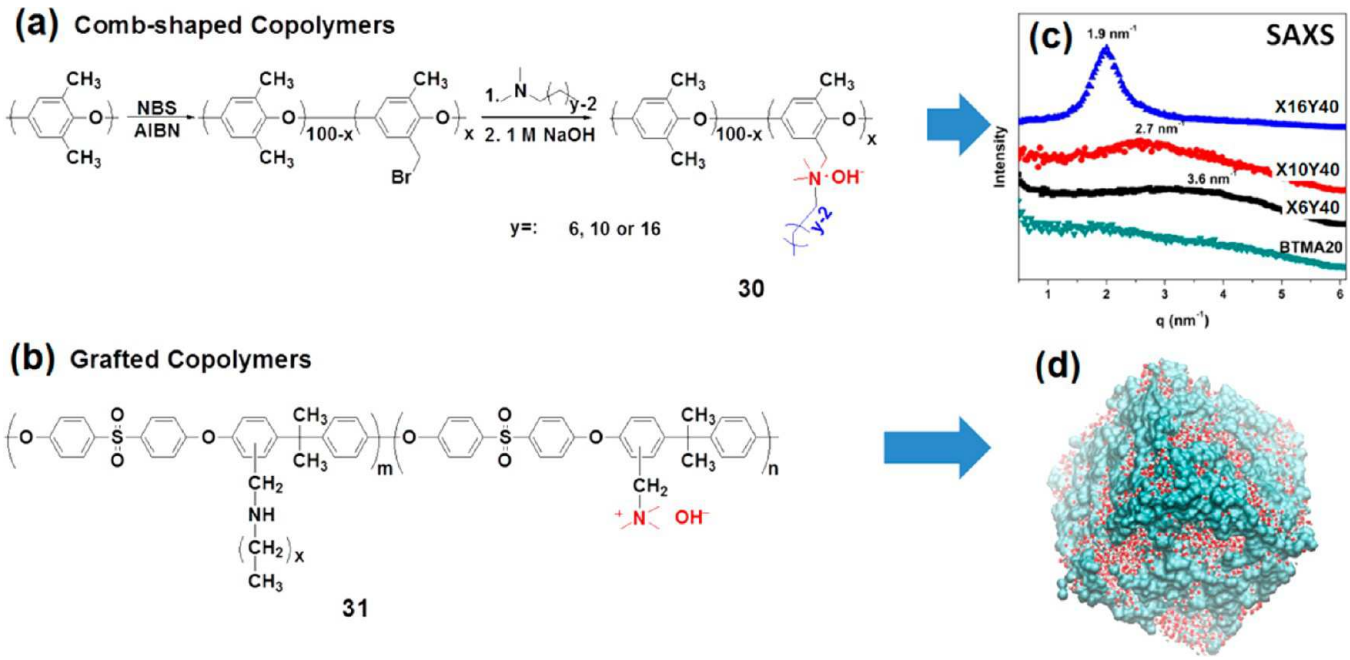

Figure 14. (a) Synthesis of comb-shaped copolymers and (c) the SAXS results in the dry state.[119] (b) Synthesis of polysulfones with grafted side chains and (d) molecular dynamics simulation.[120] Adapted with permission from refs 119 and 120.

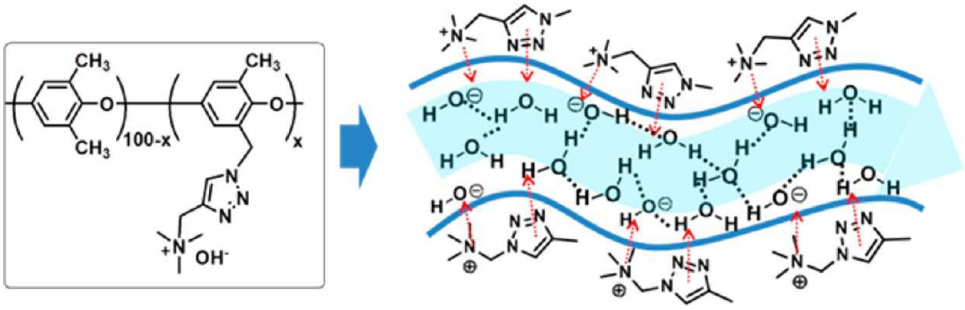

Figure 15. Possible hydrogen-bonded network and hydroxide ion hopping in AEMs with clicked 1,2,3-triazole hydroxide transport facilitator. Reproduced with permission from ref 123. Copyright 2013 Wiley.

polysulfone backbone and alkyl side chains, as shown in Figure 14d.[120] The aqueous clusters in this membrane are well connected to each other at sufficient hydration levels. Most recently, Xu and co-workers[121] reported a graft copolymer of bromomethylated poly(phenylene oxide)-*graft*-quaternized 4-vinylbenzyl chloride (BPPO-*g*-QVBC), using an activator regenerated by electron transfer for atom transfer radical polymerization (ARGET ATRP) for AEMs. Phase-separated morphology with nanosized ionic clusters embedded in the hydrophobic BPPO matrix was observed by TEM, resulting in high hydroxide conductivities of up to 100 mS/cm at 80 °C.

In addition to the construction of polymer architecture, an alternative hydroxide transport facilitator was also investigated by creating a network of hydrogen bonds for hydroxide diffusion (Figure 15). Li and co-workers[123] reported the incorporation of clicked 1,2,3-triazole as a hydroxide transport facilitator in QA-AEMs which promoted effective ionic conduction. It was believed that the hydrogen bonds between 1,2,3-triazole and water/anion form a continuous pathway for ionic conduction and ion movement. Thus, a significantly higher conductivity (up to 10 times) was observed for obtained AEMs compared to that of the AEMs without triazole groups.

A growing momentum of research interest in AEMs is motivated by the fact that alkaline systems are able to operate without the use of platinum group metals as catalyst, which is a major economic limitation for the widespread implementation of PEM fuel cells. Although the organic cations of AEMs may have lower segregation strength from the polymer backbone compared to sulfonic acid groups, the enhancement of hydroxide conductivity could be achieved by polymer architecture, for example, block and comb-shaped copolymers. As shown in Figure 16, multiblock and comb-shape architecture as well as the clicked 1,2,3-triazole strategy lead to an obvious enhancement of hydroxide transport. The reported conductivities up to 62 mS/cm at room temperature[123] and 126 mS/cm at 60 °C[16] in water are of great interest for fuel cell applications, for which a maximum power density of 823 mW cm^{-2} has been reported.[124] However, research on AEM appears to be in its early stages relative to PEM, and there still remain a number of research challenges that must be overcome before they can be successfully applied to fuel cells. A major challenge for AEMs is the intrinsic chemical instability of the quaternary ammonium group, which leads to a decrease of the ionic conductivity and to a loss of efficiency of the system. Novel approaches to stable materials in the future should focus on new types of cations that probably employ delocalization and steric shielding of the positively charged center to mitigate nucleophlic attack by hydroxide. Some polymer backbones having promising alkaline stability (e.g., PPO, poly(phenylene), polystyrene) and those

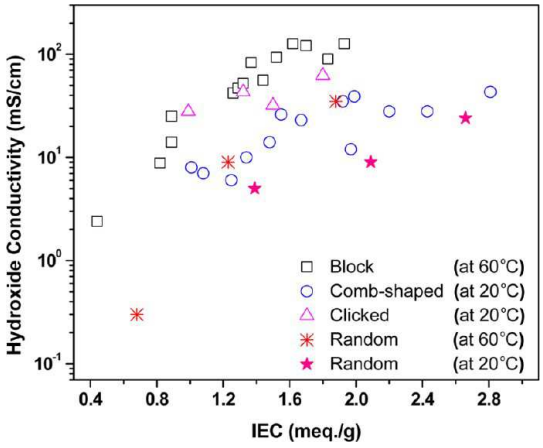

Figure 16. Performance comparison of various types of AEMs: relationship between IEC and hydroxide conductivity in water.

showing less stability (e.g., poly(arylene ether)s) and effective polymer architecture (as shown above) have been identified, but limited device testing and a rudimentary understanding of degradation mechanisms in operating devices are slowing progress on alkaline fuel cell technology. Moreover, understanding of anion transport in these complex systems is inadequate, requiring additional work on AEM polymers, especially to address anion transport mechanisms as well as chemical and mechanical stability. At the current stage of development, however, AEMs have an immediate potential application for vanadium redox-flow battery, which is discussed later.

4. APPLICATIONS

In the previous sections, we have described effective approaches toward nanochannel formation in ion-containing aromatic polymer membranes by block and comb-shaped/graft architecture, localization, sequencing or clustering of ionic groups, or the introduction of extreme polarity differences by the use of superacidic fluorosulfonic side chains. This section surveys the applications of these phase-separated polymer membranes in proton exchange membrane hydrogen fuel cells, direct methanol fuel cells, and anion exchange membrane fuel cells (Figure 17) as well as other electrochemical devices.

4.1. Proton Exchange Membrane Fuel Cells. In the proton exchange membrane fuel cell (PEMFC), the PEM requires characteristics of chemical and mechanical stability over a range of temperatures and humidities and must also exhibit sufficient proton conductivity at low water content.[1,12] In a PEMFC, the catalyst is typically coated with a very thin

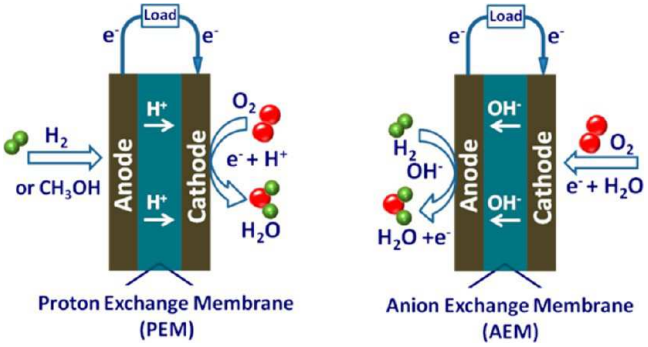

Figure 17. Schematic and half-reactions of the proton exchange membrane fuel cell (left) and the anion exchange membrane fuel cell.

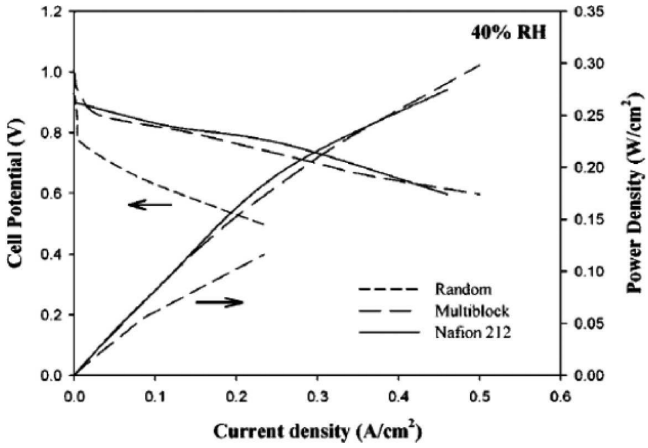

Figure 18. Hydrogen–air fuel cell performance of random and multiblock **3** aromatic copolymers and Nafion 212 membranes at 100 °C with humidification at 40%. Reproduced with permission from ref 49.

layer of PFSA ionomer, which serves to hold the catalyst in place and which acts as an ion conductor, and allows some electrical conduction. In contrast with their primary role as PEMs, PFSA ionomers have the advantage of high fuel (hydrogen or methanol) or air permeability, allowing ready access to the anode or cathode catalyst layers. When aromatic hydrocarbon ion exchange membranes are used in conjunction with catalyst-coated PFSA ionomer, a dimensional mismatch can potentially occur.[111−113] It is likely that this is a contributory factor to the often observed lower performance of hydrocarbon membranes used in fuel cells. There are numerous advantages to operating the fuel cell at higher temperature and lower humidities, such as increasing catalytic activity, reducing cathode flooding, and reducing the need for external humidification equipment.[1,14] Certain phase-separated aromatic PEMs with interconnected ion transport nanochannels showed improved proton conductivity at elevated temperature and lower RH as discussed above and are thus expected to improve fuel cell performance at higher temperature and lower RH.

At 80 °C and 90% RH, Yoshimura et al.[96] demonstrated comparable hydrogen/air fuel cell performance to that of Nafion using phase-separated aromatic PEM based on **21** having superacid groups. Although the in-plane proton conductivity of **21** (77 mS/cm at 80 °C under 90% RH) is lower than that of Nafion (89 mS/cm), the maximum power density of an MEA based on **21** (~800 mW/cm^2) was similar to Nafion. At a higher temperature (100 °C) and a lower RH, a comparison was drawn between various polymer architecture, including random copolymer PEMs and multiblock aromatic PEMs, for hydrogen/air fuel cell performance.[49] When the inlet gases were both maintained at high RH (>70% RH), the random and multiblock PEMs **3** performed similarly in single cell. However, at a lower RH of 40%, the performance of the random copolymer suffered significantly, whereas the multiblock copolymer **3** maintained performance comparable to Nafion, as shown in Figure 18. This superior performance for a hydrocarbon PEM at low RH was attributed to the multiblock copolymer's excellent proton transport properties that arise from it is morphological structure of interconnected hydrophilic nanochannels.

Watanabe,[128,129] Okamoto,[65,130] and co-workers reported fuel cell tests of phase-separated aromatic PEMs at elevated temperature and low RH. With decreasing gas humidification, the PEMFC performance of multiblock copolymers showed a much smaller reduction in fuel cell performance than comparable random copolymers. For example, the highly sulfonated multiblock copolymer **4** membrane showed acceptable fuel cell performance in a single cell of hydrogen/air fuel cell at 100 °C.[130,131] At a cell voltage of 0.6 V, the current density was 250 mA/cm^2 at 30% RH and 410 mA/cm^2 at 53% RH, confirming the operability of multiblock copolymers under conditions of elevated temperature and reduced humidity levels. Okamoto and co-workers[65,130] further reported the hydrogen/air fuel cell performance of multiblock copolymer at very low RH. The single cell performance could be maintained at a high level at 30% RH ($V_{0.5A}$: 0.70 V and W_{max}: 790 mW/cm^2) which was much higher than those of the Nafion 112 membranes at 30% RH (for example, $V_{0.5A}$ of 0.70 V and W_{max} of 610 mW/cm^2). Even at 17% RH, this multiblock copolymer membrane also shown good fuel cell performance ($V_{0.5A}$: 0.69 V and W_{max}: 730 mW/cm^2). The PEMFC derived from a multiblock poly(phenylene) copolymer[65,132] was operated for a durability test under a constant load current density of 0.5 A/cm^2 at 90 °C, 0.2 MPa, and 50% RH. After 750 h, the polarization and power output curves were compared to those before the test. No significant change in the PEMFC performance was observed, suggesting fairly high durability under PEMFC operation at high temperature and low RH operation conditions. Watanabe and co-workers reported the hydrogen fuel cell performance using sulfonated multiblock polybenzophenone/poly(arylene ether) membrane as PEM.[67] The humidity dependence of the fuel cell performance of this membrane was smaller than that of Nafion. The membrane was durable in the open circuit voltage (OCV) test at low humidity for 1100 h with minor losses in the cell voltage, which is better than that of Nafion, as shown in Figure 19.

Above 100 °C, nanophase-separated aromatic PEMs have also been shown to be effective for hydrogen/air fuel cell operation. Wang and co-workers[102] reported the hydrogen/air fuel cell performance of poly(arylene ether) **27** with superacid groups at 120 °C. The maximum power density and current density at 0.5 V of **27** were 30% and 43% higher, respectively, than those of Nafion. Recently, the width of the conducting nanochannels has been shown to have some bearing on the performance of PEMs operating at elevated temperatures and reduced humidity conditions. It is postulated that narrow channels of 2−5 nm width exhibit a capillary retention effect,[57,131] which supports water retention under low RH conditions intended for medium temperature fuel cell

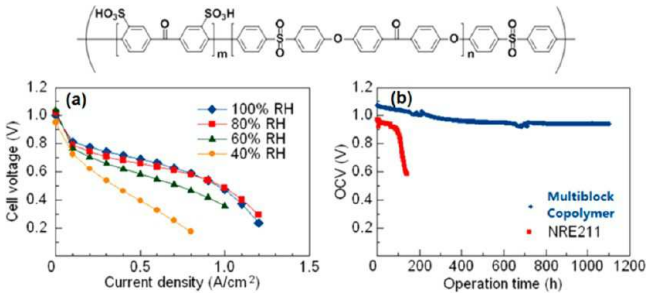

Figure 19. (a) Steady state H_2/air fuel cell performance of sulfonated multiblock polybenzophenone/poly(arylene ether) membrane (IEC = 2.57 mequiv/g) at 80 °C with humidification at 40, 60, 80, and 100% RH for both electrodes. (b) Time course of open circuit voltage (OCV) of a fuel cell with **3** (IEC = 2.57 mequiv/g) and Nafion NRE 211 membranes at 80 °C and 20% RH. Reproduced with permission from ref 67.

applications. Comparison of a clustered fluorene-based sulfonated poly(arylene ether sulfone) copolymers with four flexible pendent butylsulfonic acid units per repeat unit (**20**)[131] with a random and block copolymer showed that the clustered PEM gave relatively high cell performance (W_{max} ~ 280 mW/cm^2) at 120 °C and 35% RH compared with the random and block copolymers (W_{max} ~ 80 mW/cm^2).

Most of the cases involving nanochannel formation leading to good fuel cell performance have been achieved through block, graft, clustered, or superacidic side chains. However, nanochannels have been induced by morphological transformation during thermal cross-linking of sulfonated poly(phenylene sulfide nitrile) random copolymer.[132] The resulting network PEM exhibited membrane proton conductivity that was 160% higher than that of Nafion 212 at 80 °C and 50% RH. The network PEM with the best fuel cell performance exhibited a wormlike morphology with bicontinuous hydrophilic and hydrophobic networks of narrow diameter ranges of 15−20 and 20−25 nm, respectively. At 0.6 V, its current density and maximum power density (>900 mW/cm^2, H_2/O_2, 80 °C and 50% RH) were ~150% higher than those of Nafion 212.

4.2. Direct Methanol Fuel Cells (DMFCs). One key limitation of direct methanol fuel cell operation is high methanol permeability in currently employed ion-containing polymer membranes, especially PFSAs, which contributes to mixed potentials and low overall cell power and efficiency. Although common sulfonated polymers exhibit the desired high conductivities in water, these materials also possess undesired high methanol permeabilities. Therefore, low methanol fuel concentrations of ~1−2 M are typically fed to the anode because methanol flux increases significantly with concentration.[133] In sulfonated copolymers, many investigations reveal that proton and methanol transport increase or decrease in tandem due to the coupled nature of IEC and water uptake, making it difficult to achieve high selectivities at high proton conductivities. A compilation and analysis of literature data using nontraditional length-scale parameters provides important insights into molecular design aspects of sulfonated PEMs for DMFCs.[134,135] The performance of sulfonated PEMs in DMFCs shows that among several approaches, cross-linked systems tend to exhibit both high selectivity and conductivity, while random copolymer PEMs show a trade-off.

Comb-shaped aromatic copolymer membranes **10**[60] with low IEC (1.2 mequiv/g) were investigated for DMFC application. The initial performance of the MEAs was comparable or higher than that of a random aromatic copolymer MEA, even at high methanol concentrations, in spite of the relative lower proton conductivity (43 mS/cm). For example, the power density of the MEA using comb-shaped copolymer **10** at 350 mA/cm^2 and 0.5 M methanol was 145 mW/cm^2, whereas the power densities of MEAs using random copolymer were 136 mW/cm^2.

By replacing proton exchange membranes by anion exchange membranes in DMFCs, the direction of methanol crossover opposes that of hydroxide ion conduction, thereby mitigating or possibly eliminating this process. Therefore, more attention has recently been directed toward developing highly anion conductive AEMs for DMFCs.

4.3. Anion Exchange Membrane Fuel Cells. Anion exchange membrane fuel cells (AEMFCs) have undergone a resurgence of interest in recent years relative to PEM fuel cells[3,4] because of some important advantages when operating under alkaline conditions. These include an enhancement of electrode reaction kinetics, especially at the cathode, and cathode catalyst metals have a much higher corrosion resistance at high pH. Consequently, non-noble metals or inexpensive metal oxides can be used as catalysts in place of noble metal catalysts such as platinum. In addition, high-energy density liquids and gases such as ethanol, methanol, hydrazine, and ammonia can be adopted as fuels. Several research groups have demonstrated a working alkaline fuel cell with an anion exchange membrane using non-precious-metal catalysts to lower the cost of fuel cells.

To date, relatively few data on alkaline fuel cell performance using phase-separated aromatic AEMs with hydrophilic nanochannels have been reported. Watanabe and co-workers[16] reported a noble metal-free direct hydrazine fuel cell using multiblock copoly(arylene ether)s AEM **29**. The Ni powder and Co with poly(pyrrole) dispersed on carbon were used for the anode and the cathode, respectively. Reasonably high fuel cell performance was obtained, with the maximum power density of 161 mW/cm^2 at a current density of 446 mA/cm^2 in air and 297 mW/cm^2 at 826 mA/cm^2 in oxygen (Figure 20a). However, AEM fuel cell performance still needs considerable improvement, as does the alkali stability of AEMs in a fuel cell environment. Li and co-workers[119] employed comb-shaped copolymers **30** as ionomers in catalyst layers for alkaline fuel cells. The results indicated that the long alkyl side chain ionomer had slightly better initial performance in spite of its low IEC value, but it exhibited poor durability in the fuel cell (Figure 20b). In contrast, 90% of the initial performance was retained for the alkaline fuel cell with electrodes containing a shorter side chain after 60 h of fuel cell operation.

In most AEMFC systems, alkaline is added to the fuel to improve the power output of alkaline fuel cells. Lower ionic conductivity due to the lower ionic mobility of OH^- compared with H^+ may account for this. Although additional liquid electrolyte increases the power density of the AEMFC, the addition of alkaline electrolyte to fuel is not an optimal approach. The presence of free cations such as K^+ and Na^+ allows for the unwanted precipitation of carbonate salts, which have the potential to limit the lifetime of the AEMFC. Using fuels without the addition of KOH or NaOH would reduce the occurrence of carbonate salts, thus reducing the risk of decrease of membrane ionic conductivity caused by blockage of carbonate precipitation on or within the membrane.[3,4] This points to the need for AEMs having high ionic conductivity to

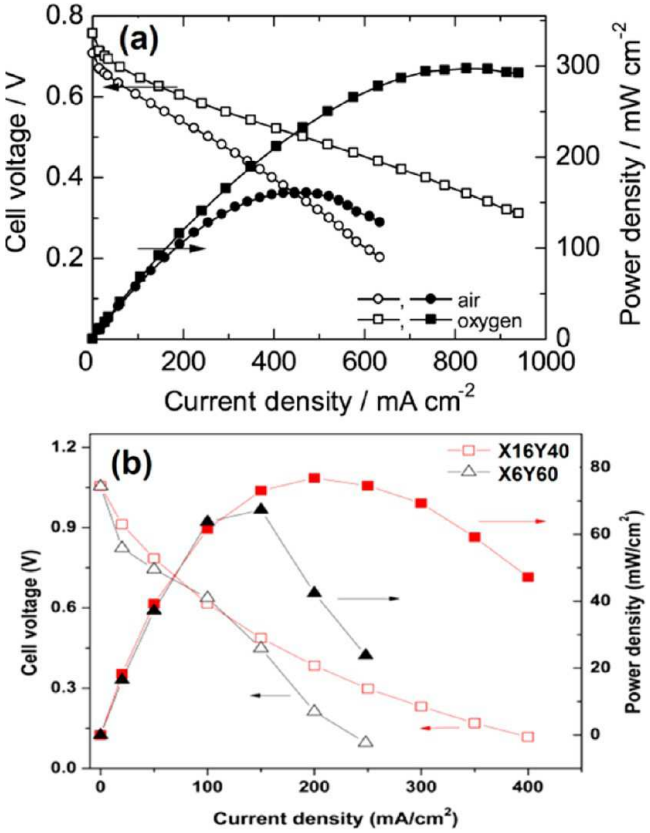

Figure 20. (a) Direct hydrazine fuel cell performance (cell voltage and power density versus current density) of a multiblock copolymer **29** (IEC = 1.93 mequiv/g) membrane[16] with air or oxygen at 80 °C (top). (b) Polarization curves and power density curves of an AEMFC with the comb-shaped ionomer **30**[119] at 50 °C with H_2/O_2 flow rate of 200/200 cm^3/min (bottom).

allow efficient transfer of OH^- produced at the cathode to the anode side and thus greatly improve the fuel cell performance.

4.4. Potential Applications in Other Electrochemical Devices. Generally, the majority of work in the design and understanding of ion-containing copolymer membranes has focused on the application needs of the hydrogen, direct methanol, and alkaline fuel cells. However, these membranes could be of significant importance in other electrochemical devices, such as water electrolysis, electrodialysis, flow batteries, artificial photosynthesis, lithium ion batteries, and microbial fuel cells. The potential application of ion-containing copolymer membranes with ion transport nanochannels in these electrochemical devices is discussed below (Figure 21).

4.4.1. Vanadium Flow Batteries (VFB). Among a wide range of energy storage techniques, vanadium flow batteries (VFBs) are regarded as efficient high-capacity energy storage devices with advantages of flexibility in design, ease of facility maintenance, and operational safety.[5] Hence, VFBs are considered to be a promising technology for large-scale applications to accommodate the demand related to energy storage, on-grid renewable energy, and smart grid. As one of the key components of VFBs, ion exchange membranes may be employed to separate positive and negative electrolytes as well as to allow selective ion transfer during the charge and discharge processes. Apart from reducing membrane cost and improving chemical stability, one of the challenging issues of research and development on VFB membranes is to reduce the

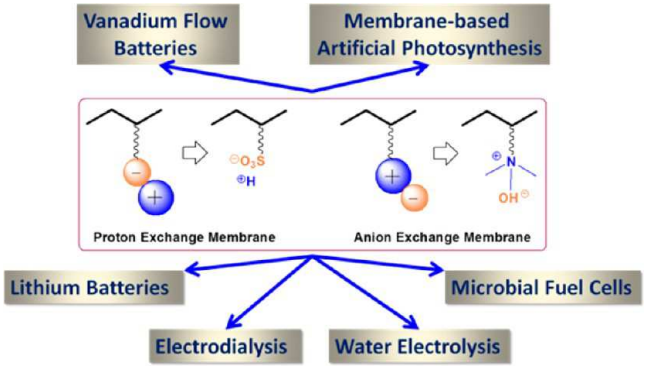

Figure 21. Potential applications of ion-containing copolymers with nanochannels in various electrochemical devices.

permeation of vanadium ions in their various oxidation states. To minimize capacity loss under operation conditions, high ion conductivity and a low permeation rate of vanadium ions or high ion selectivity are required. To date, aromatic proton exchange membranes[136,137] and anion exchange membranes[138−140] have been demonstrated to function effectively in the VFB application. In general, these membranes demonstrated better Coulombic efficiency in the VFB cell test than that of Nafion membrane,[5,141] indicating lower vanadium ion permeability. However, the long-term durability of these membranes in the $V^{(V)}$ electrolyte remains unknown. Stable ion-conductive aromatic polymer electrolyte membranes having selective ion transport nanochannels have the potential to be effective and less costly in this application.

4.4.2. Water Electrolysis. Advanced water electrolysis is one of the most efficient and reliable approaches to produce hydrogen from renewable energy such as solar, wind, and hydropower for grid-scale energy storage.[142] Polymer electrolyte membrane water electrolysis systems offer several advantages over traditional alkaline liquid electrolyte water electrolysis, which include higher energy efficiency, high pressure hydrogen production, greater hydrogen production rate, and more compact design.[143,144]

Hayes and co-workers[145] reported that microblock aromatic proton exchange membranes utilized for electrolysis exhibited good energy efficiency (1.67 V at 1 A cm^{-2} and 80 °C, corresponding to 4 kWh/N m^3 of H_2). A single cell test also showed very good electrical performance of the MEA over 62 h, yielding stable, reproducible current and voltage through repeated cell cycling. Significant enhancements in durability were achieved by utilizing an anion exchange membrane and anion conductive polymer[9,146] as the catalyst ionomer. Wang and co-workers[8] have demonstrated >500 h of operation of an alkaline membrane electrolysis device at 200 mA/cm^2 at a cell potential of below 2.25 V. The performance of the alkaline membrane device was 30−60% that of an optimized PEM electrolyzer due to ionic conduction losses being greater in AEMs as compared to PEMs. Zhuang and co-workers[9] reported water electrolysis using an anion exchange membrane and nonprecious metal catalysts, using only pure water. The initial prototype water electrolysis unit exhibited good performance comparable to that of the well-developed alkaline water electrolyzer.

However, the improvement of performance and long-term durability remain significant challenges for practical application. Thus, future improvements of membrane electrolyzers will hinge on creating highly ion-conductive, electrochemically

durable ionomers and membranes and incorporating non-precious-metal catalysts into the anode and cathode structures to achieve the goal of highly efficient, economic and durable solid-state water electrolyzers.

4.4.3. Wastewater Treatment by Electrodialysis. Electrodialysis employs an electrical current to drive cations and anions out of a water stream through cation and anion exchange membranes, respectively.[15] Desalination or deionization of wastewater by electrodialysis has some advantages over technologies such as reverse osmosis in that it is less sensitive to feedwater quality, thus reducing the need for pretreatment steps. However, the economics also depend upon the ion concentration; the higher the concentration, the greater the energy required for water deionization. Generally, electrodialysis membranes must have low electrical resistance and high ion selectivity.[132] They are typically composed of sulfonated or aminated cross-linked polystyrene, which are reinforced by blending with hydrophobic polymers or by inert mesh supports. These membranes are thick and have low conductivity due to the support structures that are necessary to maintain the mechanical integrity of the brittle polystyrene.[15,147] More advanced ion-containing aromatic copolymers having high conductivities and good mechanical properties may contribute to the development of improved electrodialysis membranes for more efficient water treatment. However, the issues relating to low ion-conductivity, fouling, chemical durability, and chlorine tolerance, which need to be solved in the future research, still apply to electrodialysis membranes.

4.4.4. Lithium Ion Batteries. Many attempts to improve the performance of lithium ion batteries have dealt with the interface problems between electrolyte and electrode, but work is now focusing on the chemical and physical properties of the electrolyte.[148−150] In particular, the replacement of flammable liquid electrolytes by solid polymer electrolyte membranes has received considerable attention recently, due to not only safety issues but also considerations of simplifying the manufacturing process and flexible design. However, the main issue in using solid polymer electrolyte membranes in lithium ion batteries arises from their relatively low ionic conductivity compared to that of liquid electrolytes.[148] Kato and co-workers[150] demonstrated that the ionic nanochannels present in copolymers can increase the Li^+ transport, which has prompted researchers to explore the role of polymer electrolyte membrane nanochannels on the Li^+ transport properties for lithium ion batteries. However, a Li^+ salt additive is still required in these systems to achieve high conductivity. When the cation required for conduction is obtained from a lithium salt, anions accumulate at the electrodes, resulting in reverse polarization that degrades battery life. A "single-ion conductor" based on a polyanionic copolymer, in which the anion was covalently bonded to the polymer chain, has been demonstrated to be effective in removing this undesirable effect.[151,152] To achieve optimal transport properties in solid polymer electrolyte membrane in the absence of additives, future research will require careful material design to maximize ion mobilities. Armand and co-workers reported a block copolymer "single-ion conductor" structure which enables an important delocalization of the negative charge.[153] Since Li^+ has weak interactions with this delocalized anionic structure, it consequently enables a high dissociation level, resulting in a relatively high ion conductivity of 1.3×10^{-5} S/cm at 60 °C.[153] Thus, single-ion conductor polymer electrolyte membranes based on ion-containing copolymers having ion-transport nanochannels and high conductivities have the potential to be integrated into next-generation lithium ion batteries.

4.4.5. Microbial Fuel Cells (MFCs). Microbial fuel cells (MFCs) use bacteria as catalysts to generate power from organic compounds. MFC technology provides a completely new approach for renewable energy generation from wastewater treatment.[154−156] Electrochemically active bacteria on the anode oxidize organic compounds under anaerobic conditions and generate electrons and protons. The electrons flow through a wire and the protons are transported to the cathode where they combine with oxygen and generate water. Single chamber membrane-free MFCs demonstrated a higher performance than other type of MFCs. However, oxygen can permeate across the cathode to the anode in membrane-free MFCs, which may inhibit the electrochemical activity of anaerobic bacteria on the anode.[154] Although a common salt bridge can be used, a more effective ion exchange channel is a PEM, which can reduce oxygen diffusion but also increase the resistance. In addition, the PEM transports cationic species other than protons as well and in MFCs concentrations of other cation species (Na^+, K^+, NH_4^+, Ca^{2+}, and Mg^{2+}) are typically 10^5 times higher than the proton concentration which resulted in an increased pH in the cathode chamber and a decreased MFC performance. Therefore, lower performance was observed when the PEMs were employed into membrane-based MFC system.[157] A PEM having nanochannels for efficient proton transport may possibly impede transport of the larger sized inorganic ions, would could improve the function of membrane-based MFC systems.

4.4.6. Membrane-Based Artificial Photosynthesis. In nature, light is harvested by photosynthesis within a fluidlike membrane, in which charge separation and relaying occur by redox reactions.[158] The membrane function is to separate the reductive and oxidative processes by efficient electron and proton transport.[159] Artificial photosynthetic systems are of interest, but research into the parameters required for efficient membranes has been little investigated. In contrast to ion conducting membranes used in fuel cell systems, membranes for photosynthetic systems need ion conductivity for ion transport associated with redox processes in addition to electron conductivity associated with light absorption.[10] In membrane-based artificial photosynthetic systems, it is a difficult challenge to find single membrane materials capable of full functionality combining ion and electron transport. Freund and co-workers[10] reported composite membranes with enhanced ionic/electron conductivity from electron conductive poly(3,4-ethylenedioxythiophene)−poly(styrenesulfonate) and proton conductive Nafion, although no device performance data were given. Achieving progress in membrane-based artificial photosynthesis devices could be accomplished by developing electronically conducting polymers with lower band gaps and ion conducting polymers with lower fuel crossover.

5. OUTLOOK AND FUTURE PROSPECTS

The formation of nanochannels in ion-containing aromatic copolymers has shown that highly ion conductive membranes can be produced without compromising some other important properties such as dimensional stability, which is important for performance improvements in fuel cells and other electrochemical devices. The considerable efforts expended in recent years on phase-separated aromatic ion-containing polymer membranes have increased the understanding of structure−property relationships and nanochannel formation and resulted in the development of much improved membranes. Random

poly(arylene ether sulfone) copolymer membranes with reported fuel cell durability of 10 000 h suggest that there are prospects for alternatives to PFSA membranes.[160] However, there is a lack of long-term stability data for phase-separated aromatic copolymers under realistic electrochemical operating conditions. The electrochemical or chemical environment (for example, formation of free radicals in a fuel cell,[53] hydroxides in alkaline fuel cell,[3,4] redox in vanadium flow battery[5]) appears to degrade aromatic copolymers by a different mechanism and more readily than PFSAs. In addition, in fuel cell tests of aromatic copolymers, the situation is made more complex by interfacial compatibility issues between the membrane and the catalyst layers.[12] Among aromatic ion-containing polymers, those with extremely electron-poor backbones such as poly(phenylene sulfone)s[53] and poly(phenylene)s[161] have been shown to be the most hydrolytically and thermooxidatively stable due to the absence of any electron-donating groups such as ether linkages. These polymer backbones are likely to have the necessary stability for new-generation proton exchange membranes and anion exchange membranes. However, poly(phenylene sulfone)s and poly(phenylene)s have high degrees of chain rigidity, which may severely compromise mechanical properties as discussed above, so new designs of these polymers must incorporate functionality or side chains to improve interchain interactions or chain entanglement.

Inducing nanochannel formation for proton transport in these new generations of proton exchange membranes based on block copoly(phenylene sulfone)s[52,54] or poly(phenylene)s[63−68] is beginning to be explored. Employing block copolycondensation as described previously, multiblock sulfonated poly(phenylene sulfone)s were prepared by Jannasch and Meyer.[52,54] These approaches open new research avenues toward highly proton-conductive and electrochemically/chemically stable PEM materials, but they are still at the initial stages. Therefore, more fundamental work in understanding the self-assembly and development of long-range, well-ordered morphologies of these aromatic ion-containing copolymers is needed. Complementary synthetic and simulation studies of chemically diverse polymers are needed to advance the basic knowledge surrounding materials that can withstand the electrochemical stress in various devices. Investigations into the stability (e.g., resistance to chemical, hydrolytic, and mechanical degradation) of PEMs during electrochemical device operation have not fully established the links between polymer structure and morphology and electrochemical/chemical degradation. Understanding these key issues will be necessary to achieve the durability expected of them for commercial success.

Compared to PEMs, AEM development is in its infancy, with challenges to overcome before being suitable for real applications. A number of well-defined copolymer architectures having nanochannels for anionic transport (block,[16] graft copolymers[17,119]) have been reported in the literature. For practical applications, an anionic conductivity of >50 mS cm at 80 °C needs to be achieved. In addition, although polystyrene and PPO-based AEMs have been claimed to be much more stable than aromatic poly(arylene ether) polymers under alkaline conditions,[162] the problematic durability of AEMs due to degradation of quaternary ammonium groups by S_N2 and/or Hoffmann elimination must be improved.[163,164] Oxidative degradation of AEMFCs under fuel-cell operating conditions has been another concern because of the electron-rich PS or PPO, which could be readily degraded under the electrochemical environment.[121] Synthetic and simulation methods used to prepare or improve the performance of PEM membranes can be applied to design advanced AEMs. For example, Los Alamos National Laboratory reported that a poly(phenylene)-based[165,166] AEM developed by Sandia National Laboratory had good chemical and mechanical stability (stable >670 h at 60 °C in 4 M NaOH) due to the wholly aromatic electron-deficient structure, which was better than typical poly(aryl ether)-type AEMs. High ionic conductivity (>50 mS/cm) was also achieved. The QA group on a long pendent spacer instead of a typical benzyl-type spacer resulted in no observable degradation of the ammonium groups after alkaline stability testing.[166,167] Removal of the benzyl-type spacer by direct attachment of a guanadinium-functionalized pendent phenyl group on a polysulfone AEM also led to improved stability.[168] Additionally, replacing quaternary ammonium groups with other functional groups such as phosphonium[169] could be a solution to improve the alkaline stability of functional groups, but there are limited literature reports on this topic. There is still a need and opportunities to develop AEMs with phase-separated nanochannel morphology that not only have high hydroxide ion conductivity and selectivity but also exhibit excellent electrochemical/chemical stability at high pH and elevated temperatures using thermoxidatively and hydrolytically stable poly(phenylene sulfone) and poly(phenylene) backbones. Providing a fundamental understanding of hydroxide conducting systems, elucidating and reducing the effect of carbonate formation in hydroxide conducting systems, exploring the stability and basicity of cations, and relating cation chemistry and structure to stability and conductivity are the future research challenges that may result in high performance AEMs for electrochemical device applications.

6. CONCLUSIONS

The formation of phase-separated nanochannel morphology for efficient ion conduction in aromatic copolymers has been highlighted. Specifically, block and comb-shaped/graft copolymer architecture, localized or clustered ionic groups and the introduction of superacidic groups have been shown to be effective strategies to induce the formation of phase-separated nanochannels and thus improve ion transport in the aromatic copolymer membranes. Phase-separated PEMs having nanochannel have shown to improve hydrogen/oxygen (air) fuel cell performance under reduced relative humidity and elevated temperature (>80 °C) compared to random copolymer analogues. However, high proton conductivity/methanol selectivities were less commonly reported using these approaches, which have the potential to be the new generation of membranes for DMFCs. Although AEMs are in a relatively early stage of development, phase-separated AEMs have been claimed to be promising membranes for alkaline fuel cells. It is clear that ordered nanochannel morphologies may positively influence transport properties, which can improve the performance of fuel cells and other electrochemical devices such as vanadium flow batteries, electrolysis, electrodialysis, microbial fuel cells, and membrane-based artificial photosynthesis. To realize these material advances for electrochemical devices, a more thorough fundamental investigation on morphology as well as durability for ion-containing aromatic copolymers should be pursued.

AUTHOR INFORMATION

Corresponding Author

*E-mail: michael.guiver@nrc-cnrc.gc.ca (M.D.G.).

Notes

The authors declare no competing financial interest.

Biographies

Nanwen Li received his BSc in 2004 from Northeast Normal University, China, and his PhD in organic chemistry from Changchun Institute of Applied Chemistry, Chinese Academy of Sciences, in 2009 where he worked under Professor Suobo Zhang. Subsequently, he moved to the Hanyang University where he worked with Professors M. D. Guiver and Y. M. Lee, and then in 2010 he joined the research group of Professor Binder at Martin-Luther University as a Humboldt postdoctoral fellow. After that, he moved to the National Research Council Canada and worked with Professor M. D. Guiver again. Currently, he is working with Professor William Koros at the Georgia Institute of Technology as a postdoctoral fellow. His research interests include the preparation and properties of ion exchange membrane for new energy, gas separation, and clean water.

Michael D. Guiver is a Principal Research Officer at the National Research Council Canada. He obtained his BSc from London University, his MSc from Carleton University, and his PhD from Carleton University, Ottawa, in 1988. He participated in the "world class university" (WCU) program as a visiting chair professor at Hanyang University, Seoul, Republic of Korea. He has been an Editor for the *Journal of Membrane Science* since 2009 and joined the Editorial Advisory Board of *Macromolecules* and *ACS Macro Letters* in 2013. His current research interests include polymer electrolyte membranes for fuel cell and other applications and high free-volume intrinsically microporous ladder polymers and networks for membrane gas separation applications such as carbon dioxide capture.

REFERENCES

(1) Park, C. H.; Lee, C. H.; Guiver, M. D.; Lee, Y. M. *Prog. Polym. Sci.* **2011**, *36*, 1443−1498.
(2) Wu, L.; Zhang, Z.; Ran, J.; Zhou, D.; Li, C.; Xu, T. *Phys. Chem. Chem. Phys.* **2013**, *15*, 4870−4887.
(3) Boschet, F.; Ameduri, B. *Prog. Polym. Sci.* **2011**, *36*, 1521−1557.
(4) Merle, G.; Wessling, M.; Nijmeijer, K. *J. Membr. Sci.* **2011**, *377*, 1−35.
(5) Wang, W.; Luo, Q.; Li, B.; Wei, X.; Li, L.; Yang, Z. *Adv. Funct. Mater.* **2013**, *23*, 970−986.
(6) Ma, L. R.; Sui, S.; Zhai, Y. C. *Int. J. Hydrogen Energy* **2009**, *34*, 678−984.
(7) Wei, G. Q.; Wang, Y. X.; Huang, C. D.; Gao, Q. J.; Wang, Z. T.; Xu, L. *Int. J. Hydrogen Energy* **2010**, *35*, 3951−3957.
(8) Leng, Y.; Chen, G.; Mendoza, A. J.; Tighe, T. B.; Hickner, M. A.; Wang, C. Y. *J. Am. Chem. Soc.* **2012**, *134*, 9054−9057.
(9) Xiao, L.; Zhang, S.; Pan, J.; Yang, C.; He, M.; Zhuang, L.; Lu, J. *Energy Environ. Sci.* **2012**, *5*, 7869−7871.
(10) McFarlane, S. L.; Day, B. A.; McEleney, K.; Freund, M. S.; Lewis, N. S. *Energy Environ. Sci.* **2011**, *4*, 1700−1703.
(11) Mauritz, K. A.; Moore, R. B. *Chem. Rev.* **2004**, *104*, 4535−4585.
(12) Hickner, M. A.; Ghassemi, H.; Kim, Y. S.; Einsla, B. R.; McGrath, G. E. *Chem. Rev.* **2004**, *104*, 4587−4611.
(13) Hickner, M. A. *Mater. Today* **2004**, *13*, 34−41.
(14) Peckham, T. J.; Holdcroft, S. *Adv. Mater.* **2010**, *22*, 4667−4690.
(15) Strathmann, H.; Grabowski, A.; Eigenberger, G. *Ind. Eng. Chem. Res.* **2013**, *52*, 10364−10379.
(16) Tanaka, M.; Fukasawa, K.; Nishino, E.; Yamaguchi, S.; Yamada, K.; Tanaka, H.; Miyatake, K.; Watanabe, M. *J. Am. Chem. Soc.* **2011**, *133*, 10646−10654.
(17) Li, N.; Yan, T.; Li, Z.; Thurn-Albrechtb, T.; Binder, W. H. *Energy Environ. Sci.* **2012**, *5*, 7888−7892.
(18) Kreuer, K. D.; Paddison, S. J.; Spohr, E.; Schuster, M. *Chem. Rev.* **2004**, *104*, 4637−4678.
(19) Agmon, N. *Chem. Phys. Lett.* **1995**, *244*, 456−462.
(20) Kreuer, K. D. *Solid State Ionics* **2000**, *136−137*, 149−160.
(21) Dippel, T.; Kreuer, K. D. *Solid State Ionics* **1991**, *46*, 3−9.
(22) Sone, Y.; Ekdunge, P.; Simonsson, D. *J. Electrochem. Soc.* **1996**, *143*, 1254−1259.
(23) Steininger, H.; Schuster, M.; Kreuer, K. D.; Kaltbeitzel, A.; Bingol, B.; Meyer, W. H.; Schauff, S.; Brunklaus, G.; Maier, J.; Spiess, H. W. *Phys. Chem. Chem. Phys.* **2007**, *9*, 1764−1773.
(24) Li, N.; Wang, C.; Lee, S. Y.; Park, C. H.; Lee, Y. M.; Guiver, M. D. *Angew. Chem., Int. Ed.* **2011**, *50*, 9158−9161.
(25) Lingwood, M. D.; Zhang, Z.; Kidd, B. E.; McCreary, K. B.; Hou, J.; Madsen, L. A. *Chem. Commun.* **2013**, *49*, 4283−4285.
(26) de Araujo, C. C.; Kreuer, K. D.; Schuster, M.; Portale, G.; Mendil-Jakani, H.; Gebel, G.; Maier, J. *Phys. Chem. Chem. Phys.* **2009**, *11*, 3305−3312.
(27) Li, J.; Park, J. K.; Moore, R. B.; Madsen, L. A. *Nat. Mater.* **2011**, *10*, 501−511.
(28) Park, J. K.; Li, J.; Divoux, G. M.; Madsen, L. A.; Moore, R. B. *Macromolecules* **2011**, *44*, 5701−5710.
(29) Hou, J.; Li, J.; Madsen, L. A. *Macromolecules* **2010**, *43*, 347−353.
(30) Nakano, T.; Nagaoka, S.; Kawakami, H. *Polym. Adv. Technol.* **2005**, *16*, 753−757.
(31) Marestin, C.; Gebel, G.; Diat, O.; Mercier, R. *Adv. Polym. Sci.* **2008**, *216*, 185−258.
(32) Jouanneau, J.; Mercier, R.; Gonon, L.; Gebel, G. *Macromolecules* **2007**, *40*, 983−990.
(33) Li, Q.; Jensen, J. O.; Savinell, R. F.; Bjerrum, N. J. *Prog. Polym. Sci.* **2009**, *34*, 449−477.
(34) Xu, K.; Li, K.; Khanchaitit, P.; Wang, Q. *Chem. Mater.* **2007**, *19*, 5937−5945.
(35) Gao, J.; Yang, Y.; Lee, D.; Holdcroft, S.; Frisken, B. J. *Macromolecules* **2006**, *39*, 8060−8066.
(36) Dorenbos, G.; Morohoshi, K. *Energy Environ. Sci.* **2010**, *3*, 1326−1338.
(37) Elabd, Y. A.; Hickner, M. A. *Macromolecules* **2011**, *44*, 1−11.

(38) Chan, K. P.; Argyropoulos, D. S.; White, D. M.; Yeagers, G. W.; Hay, A. S. *Macromolecules* **1994**, *27*, 6371−6375.
(39) Lee, H. S.; Roy, A.; Lane, O.; Dunn, S.; McGrath, J. E. *Polymer* **2008**, *49*, 715−723.
(40) Nakabayashi, K.; Matsumoto, K.; Ueda, M. *J. Polym. Sci., Part A: Polym. Chem.* **2008**, *46*, 3947−3957.
(41) Nakabayashi, K.; Matsumoto, K.; Ueda, M. *J. Polym. Sci., Part A: Polym. Chem.* **2008**, *46*, 7332−7341.
(42) Lee, H. S.; Badami, A. S.; Roy, A.; McGrath, J. E. *J. Polym. Sci., Part A: Polym. Chem.* **2007**, *45*, 4879−4890.
(43) Bae, B.; Yoda, T.; Miyatake, K.; Uchida, H.; Watanabe, M. *Angew. Chem., Int. Ed.* **2010**, *49*, 317−320.
(44) Ghassemi, H.; McGrath, J. E.; Zawodzinski, T. A. *Polymer* **2006**, *47*, 4132−4139.
(45) Fan, Y.; Cornelius, C. J.; Lee, H. S.; McGrath, J. E.; Zhang, M.; Moore, R.; Staiger, C. L. *J. Membr. Sci.* **2013**, *430*, 106−112.
(46) Roy, A.; Hickner, M. A.; Yu, X.; Li, Y.; Glass, T. E.; McGrath, J. E. *J. Polym. Sci., Part A: Polym. Chem.* **2006**, *44*, 2226−2239.
(47) Nberger, F. S.; Kerres, J. *J. Polym. Chem., Part A: Polym. Chem.* **2007**, *45*, 5237−5255.
(48) Takamuku, S.; Jannasch, P. *Adv. Energy Mater.* **2012**, *2*, 129−140.
(49) Einsla, M. L.; Kim, Y. S.; Hawley, M.; Lee, H. S.; McGrath, J. E.; Liu, B.; Guiver, M. D.; Pivovar, B. S. *Chem. Mater.* **2008**, *20*, 5636−5642.
(50) Bae, B.; Miyatake, K.; Watanabe, M. *Macromolecules* **2010**, *43*, 2684−2691.
(51) Nakabayashi, K.; Higashihara, T.; Udea, M. *J. Polym. Sci., Part A: Polym. Chem.* **2010**, *48*, 2757−2764.
(52) Takamuku, S.; Jannasch, P. *Macromolecules* **2012**, *45*, 6538−6546.
(53) Schuster, M.; Kreuer, K. D.; Andersen, H. T.; Maier, J. *Macromolecules* **2007**, *40*, 598−607.
(54) Titvinidze, G.; Kreuer, K. D.; Schuster, M.; de Araujo, C. C.; Melchior, J. P.; Meyer, W. H. *Adv. Funct. Mater.* **2012**, *22*, 4456−4470.
(55) Miyatake, K.; Hirayama, D.; Bae, B.; Watanabe, M. *Polym. Chem.* **2012**, *3*, 2517−2522.
(56) Kim, T. A.; Jo, W. H. *Chem. Mater.* **2010**, *22*, 3646−3652.
(57) Park, M. J.; Downing, K. H.; Jackson, A.; Gomez, E. D.; Minor, A. M.; Cookson, D.; Weber, A. Z.; Balsara, N. P. *Nano Lett.* **2007**, *7*, 3547−3552.
(58) Saito, T.; Moore, H. D.; Hickner, M. A. *Macromolecules* **2010**, *43*, 599−601.
(59) Borup, R.; Meyers, J.; Pivovar, B.; Kim, Y. S.; Mukundan, R.; Garland, N.; Myers, D.; Wilson, M.; Garzon, F.; Wood, D.; Zelenay, P.; More, K.; Stroh, K.; Zawodzinski, T.; Boncella, J.; McGrath, J. E.; Inaba, M.; Miyatake, K.; Hori, M.; Ota, K.; Ogumi, Z.; Miyata, S.; Nishikata, A.; Siroma, Z.; Uchimoto, Y.; Yasuda, K.; Kimijima, K.; Iwashita, N. *Chem. Rev.* **2007**, *107*, 3904−3951.
(60) Kim, D. S.; Kim, Y. S.; Guiver, M. D.; Ding, J.; Pivovar, B. S. *J. Power Sources* **2008**, *182*, 100−105.
(61) Li, N.; Lee, S. Y.; Liu, Y. L.; Lee, Y. M.; Guiver, M. D. *Energy Environ. Sci.* **2012**, *5*, 5346−5355.
(62) Hay, A. S. *Macromolecules* **1969**, *2*, 107.
(63) Si, K.; Dong, D.; Wycisk, R.; Litt, M. *J. Mater. Chem.* **2012**, *22*, 20907−20917.
(64) Si, K.; Wycisk, R.; Dong, D.; Cooper, K.; Rodgers, M.; Brooker, P.; Slattery, D.; Litt, M. *Macromolecules* **2013**, *46*, 422−433.
(65) Chen, S.; Hara, R.; Chen, K.; Zhang, X.; Endo, N.; Higa, M.; Okamoto, K. I.; Wang, L. *J. Mater. Chem. A* **2013**, *1*, 8178−8189.
(66) Umezawa, K.; Oshima, T.; Yoshizawa-Fujita, M.; Takeoka, Y.; Rikukawa, M. *ACS Macro Lett.* **2012**, *1*, 969−972.
(67) Miyahara, T.; Hayano, T.; Matsuno, S.; Watanabe, M.; Miyatake, K. *ACS Appl. Mater. Interfaces* **2012**, *4*, 2881−2884.
(68) Zhang, X.; Sheng, L.; Higashihara, T.; Ueda, M. *Polym. Chem.* **2013**, *4*, 1235−1242.
(69) Tsang, E. M. W.; Zhang, Z.; Shi, Z.; Soboleva, T.; Holdcroft, S. *J. Am. Chem. Soc.* **2007**, *129*, 15106−15107.
(70) Norsten, T. B.; Guiver, M. D.; Murphy, J.; Astill, T.; Navessin, T.; Holdcroft, S.; Frankamp, B. L.; Rotello, V. M.; Ding, J. *Adv. Funct. Mater.* **2006**, *16*, 1814−1822.
(71) Nieh, M. P.; Guiver, M. D.; Kim, D. S.; Ding, J. F.; Norsten, T. *Macromolecules* **2008**, *41*, 6176−6182.
(72) Dimitrov, I.; Takamuku, S.; Jankova, K.; Jannasch, P.; Hvilsted, S. *Macromol. Rapid Commun.* **2012**, *33*, 1368−1374.
(73) Guiver, M. D.; Robertson, G. P.; Yoshikawa, M.; Tam, C. M. *ACS Symp. Ser.* **1999**, *744*, Chapter 10, pp 137−161.
(74) Parvole, J.; Jannasch, P. *Macromolecules* **2008**, *41*, 3893−3903.
(75) Ingratta, M.; Elomaab, M.; Jannasch, P. *Polym. Chem.* **2010**, *1*, 739−746.
(76) Ingratta, M.; Jutemar, E. P.; Jannasch, P. *Macromolecules* **2011**, *44*, 2074−2083.
(77) Matsumura, S.; Hlil, A. R.; Lepiller, C.; Gaudet, J.; Guay, D.; Shi, Z.; Hay, A. S. *Macromolecules* **2008**, *41*, 281−284.
(78) Matsumura, S.; Hlil, A. R.; Lepiller, C.; Gaudet, J.; Guay, D.; Hay, A. S. *Macromolecules* **2008**, *41*, 277−280.
(79) Matsumura, S.; Hlil, A. R.; Du, N.; Lepiller, C.; Gaudet, J.; Guay, D.; Hay, A. S. *J. Polym. Sci., Part A: Polym. Chem.* **2008**, *46*, 3860−3868.
(80) Matsumura, S.; Hlil, A. R.; Hay, A. S. *J. Polym. Sci., Part A: Polym. Chem.* **2008**, *46*, 6365−6375.
(81) Matsumoto, K.; Higashihara, T.; Ueda, M. *Macromolecules* **2009**, *42*, 1161−1166.
(82) Tian, S.; Meng, Y.; Hay, A. S. *Macromolecules* **2009**, *42*, 1153−1160.
(83) Li, N.; Shin, D. W.; Hwang, D. S.; Lee, Y. M.; Guiver, M. D. *Macromolecules* **2010**, *43*, 9810−9820.
(84) Simon, S.; Espuche, E.; Gouanve, F.; Chauveau, E.; Marestin, C.; Mercier, R. *J. Phys. Chem. B* **2012**, *116*, 12750−12759.
(85) Takamuku, S.; Weiber, E. A.; Jannasch, P. *ChemSusChem* **2013**, *6*, 308−319.
(86) Weiber, E. A.; Takamuku, S.; Jannasch, P. *Macromolecules* **2013**, *46*, 3476−3485.
(87) Matsumoto, K.; Higashihara, T.; Ueda, M. *J. Polym. Sci., Part A: Polym. Chem.* **2009**, *47*, 3444−3453.
(88) Wang, C.; Li, N.; Shin, D. W.; Lee, S. Y.; Kang, N. R.; Lee, Y. M.; Guiver, M. D. *Macromolecules* **2011**, *44*, 7296−7306.
(89) Wang, C.; Shin, D. W.; Lee, S. Y.; Kang, N. R.; Robertson, G. P.; Lee, Y. M.; Guiver, M. D. *J. Mater. Chem.* **2012**, *22*, 25093−25101.
(90) Liu, B.; Robertson, G. P.; Kim, D.-S.; Guiver, M. D.; Hu, W.; Jiang, Z. *Macromolecules* **2007**, *40*, 1934−1944.
(91) Liu, B.; Robertson, G. P.; Kim, D.-S.; Sun, X.; Jiang, Z.; Guiver, M. D. *Polymer* **2010**, *51*, 403−413.
(92) Li, N.; Hwang, D. S.; Lee, S. Y.; Liu, Y. L.; Lee, Y. M.; Guiver, M. D. *Macromolecules* **2011**, *44*, 4901−4910.
(93) Stewart, R. In *The Proton: Applications to Organic Chemistry*; Academic Press: Orlando, FL, 1985; p 134.
(94) Kreuer, K. D. *J. Membr. Sci.* **2001**, *185*, 29−39.
(95) Cho, C. G.; Kim, Y. S.; Yu, X.; Hill, M.; McGrath, J. E. *J. Polym. Sci., Part A: Polym. Chem.* **2006**, *44*, 6007−6014.
(96) Yoshimura, K.; Iwasaki, K. *Macromolecules* **2009**, *42*, 9302−9306.
(97) Miyatake, K.; Shimura, T.; Mikamiac, T.; Watanabe, M. *Chem. Commun.* **2009**, 6403−6405.
(98) Mikami, T.; Miyatake, K.; Watanabe, M. *ACS Appl. Mater. Interfaces* **2010**, *2*, 1714−1721.
(99) Mikami, T.; Miyatake, K.; Watanabe, M. *J. Polym. Sci., Part A: Polym. Chem.* **2011**, *49*, 452−464.
(100) Nakabayashi, K.; Higashihara, T.; Ueda, M. *Macromolecules* **2011**, *44*, 1603−1609.
(101) Nakagawa, T.; Nakabayashi, K.; Higashihara, T.; Ueda, M. *J. Polym. Sci., Part A: Polym. Chem.* **2011**, *49*, 2997−3003.
(102) Xu, K.; Oh, H.; Hickner, M. A.; Wang, Q. *Macromolecules* **2011**, *44*, 4605−4609.
(103) Chang, Y.; Brunello, G. F.; Fuller, J.; Hawley, M.; Kim, Y. S.; Disabb-Miller, M.; Hickner, M. A.; Jang, S. S.; Bae, C. *Macromolecules* **2011**, *44*, 8458−8469.

(104) Shin, D. W.; Lee, S. Y.; Lee, C. H.; Lee, K. S.; Park, C. H.; McGrath, J. E.; Zhang, M.; Moore, R. B.; Lingwood, M. D.; Madsen, L. D.; Kim, Y. T.; Hwang, I.; Lee, Y. M. *Macromolecules* **2013**, *46*, 7797−804.
(105) Schuster, M.; de Araujo, C. C.; Atanasov, V.; Andersen, F.; Kreuer, K. D.; Maier, J. *Macromolecules* **2009**, *42*, 3129−3137.
(106) Matsumoto, K.; Nakagawa, T.; Higashihara, T.; Ueda, M. *J. Polym. Sci., Part A: Polym. Chem.* **2009**, *47*, 5827−5834.
(107) Nakagawa, T.; Nakabayashi, K.; Higashihara, T.; Ueda, M. *J. Mater. Chem.* **2010**, *20*, 6662−6667.
(108) Dean, J. A. *Lange's Handbook of Chemistry*, 15th ed.; McGraw-Hill: New York, 1999.
(109) Vanysek, P. Ionic Conductivity and Diffusion at Infinite Dilution. In *CRC Handbook of Chemistry and Physics*, 83rd ed.; Lide, D. R., Ed.; CRC Press: Boca Raton, FL, 2002.
(110) Zhang, Z. C.; Chalkova, E.; Fedkin, M.; Wang, C.; Lvov, S. N.; Komarneni, S.; Chung, T. C. *Macromolecules* **2008**, *41*, 9130−9139.
(111) Grew, K. N.; Chiu, W. K. S. *J. Electrochem. Soc.* **2010**, *157*, B327−B337.
(112) Marx, D. *ChemPhysChem* **2006**, *7*, 1848−1870.
(113) Choi, P.; Jalani, N. H.; Datta, R. *J. Electrochem. Soc.* **2005**, *152*, E84−E89.
(114) Asthagiri, D.; Pratt, L. R.; Kress, J. D.; Gomez, M. A. *Proc. Natl. Acad. Sci. U. S. A.* **2004**, *101*, 7229−7233.
(115) Agmon, N. *Chem. Phys. Lett.* **2000**, *319*, 247−252.
(116) Jasti, A.; Shahi, V. K. *J. Mater. Chem. A* **2013**, *1*, 6134−6137.
(117) Park, D. Y.; Kohl, P. A.; Beckham, H. W. *J. Phys. Chem. C* **2013**, *117*, 15468−15477.
(118) Zhao, Z.; Wang, J.; Li, S.; Zhang, S. *J. Power Sources* **2011**, *196*, 4445−4450.
(119) Li, N.; Leng, Y.; Hickner, M. A.; Wang, C. Y. *J. Am. Chem. Soc.* **2013**, *135*, 10124−10133.
(120) Pan, J.; Chen, C.; Zhuang, L.; Lu, J. *Acc. Chem. Res.* **2012**, *45*, 473−481.
(121) Ran, J.; Wu, L.; Xu, T. *Polym. Chem.* **2013**, *4*, 4612−4620.
(122) Li, N.; Zhang, Q.; Wang, C.; Lee, Y. M.; Guiver, M. D. *Macromolecules* **2012**, *45*, 2411−2419.
(123) Li, N.; Guiver, M. D.; Binder, W. H. *ChemSusChem* **2013**, *6*, 1376−1383.
(124) Mamlouk, M.; Horsfall, J.; Williams, C.; Scott, K. *Int. J. Hydrogen Energy* **2012**, *37*, 11912−11920.
(125) Kim, Y. S.; Pivovar, B. S. *J. Electrochem. Soc.* **2010**, *157*, B1616−B1623.
(126) Kim, Y. S.; Pivovar, B. S. *Annu. Rev. Chem. Biomol. Eng.* **2010**, *1*, 123−148.
(127) Kim, Y. S.; Einsla, M.; McGrath, J. E.; Pivovar, B. S. *J. Electrochem. Soc.* **2010**, *157*, B1602−B1607.
(128) Bae, B.; Miyatake, K.; Uchida, M.; Uchida, H.; Sakiyama, Y.; Okanishi, T.; Watanabe, M. *ACS Appl. Mater. Interfaces* **2011**, *3*, 2786−2793.
(129) Bae, B.; Yoda, T.; Miyatake, K.; Uchida, M.; Uchida, H.; Watanabe, M. *J. Phys. Chem. B* **2010**, *114*, 10481−10487.
(130) Chen, S.; Chen, K.; Zhang, X.; Hara, R.; Endo, N.; Higa, M.; Okamoto, K.; Wang, L. *Polymer* **2013**, *54*, 236−245.
(131) Lee, S. Y.; Shin, D. W.; Wang, C. Y.; Lee, K. H.; Guiver, M. D.; Lee, Y. M. *Electrochem. Commun.* **2013**, *31*, 120−124.
(132) Lee, S. Y.; Kang, N. R.; Shin, D. W.; Lee, C. H.; Lee, K. S.; Guiver, M. D.; Lee, Y. M. *Energy Environ. Sci.* **2012**, *5*, 9795−9802.
(133) Ge, J.; Liu, H. *J. Power Sources* **2005**, *142*, 56−69.
(134) Pivovar, B. S.; Wang, Y. X.; Cussler, E. L. *J. Membr. Sci.* **1999**, *154*, 155−162.
(135) Kim, Y. S.; Kim, D. S.; Guiver, M. D.; Pivovar, B. S. *J. Membr. Sci.* **2011**, *374*, 49−58.
(136) Chen, D.; Wang, S.; Xiao, M.; Meng, Y. *Energy Environ. Sci.* **2010**, *3*, 622−628.
(137) Mai, Z.; Zhang, H.; Li, X.; Xiao, S.; Zhang, H. *J. Power Sources* **2011**, *196*, 5737−5741.
(138) Zhang, H.; Zhang, H.; Li, X.; Mai, Z.; Zhang, J. *Energy Environ. Sci.* **2011**, *4*, 1676−1679.
(139) Mai, Z.; Zhang, H.; Zhang, H.; Xu, W.; Wei, W.; Na, H.; Li, X. *ChemSusChem* **2013**, *6*, 328−335.
(140) Chen, D.; Hickner, M. A.; Agar, A.; Kumbur, E. C. *ACS Appl. Mater. Interfaces* **2013**, *5*, 7559−7566.
(141) Zhang, H.; Zhang, H.; Li, X.; Mai, Z.; Wei, W. *Energy Environ. Sci.* **2012**, *5*, 6299−6303.
(142) Williams, J. H.; DeBenedictis, A.; Ghanadan, R.; Mahone, A.; Moore, J.; Morrow, W. R.; Price, S.; Torn, M. S. *Science* **2012**, *335*, 53−59.
(143) Grigoriev, S. A.; Porembsky, V. I.; Fateev, V. N. *Int. J. Hydrogen Energy* **2006**, *31*, 171−175.
(144) Marshall, A. T.; Sunde, S.; Tsypkin, M.; Tunold, R. *Int. J. Hydrogen Energy* **2007**, *32*, 2320−2324.
(145) Smith, D. W.; Oladoyinbo, F. O.; Mortimore, W. A.; Colquhoun, H. M.; Thomassen, M. S.; OdegArd, A.; Guillet, N.; Mayousse, E.; Klicpera, T.; Hayes, W. *Macromolecules* **2013**, *46*, 1504−1511.
(146) Charcosset, C. *Desalination* **2009**, *245*, 214−231.
(147) Goodenough, J. B.; Kim, Y. *Chem. Mater.* **2010**, *22*, 587−603.
(148) Hammami, A.; Raymond, N.; Armand, M. *Nature* **2003**, *424*, 635−636.
(149) Marzantowicz, M.; Dygas, J. R.; Krok, F.; Florjczyk, Z.; Zygado-Monikowska, E. *Electrochim. Acta* **2007**, *53*, 1518−1526.
(150) Ichikawa, T.; Yoshio, M.; Hamasaki, A.; Kagimoto, J.; Ohno, H.; Kato, T. *J. Am. Chem. Soc.* **2011**, *133*, 2163−2169.
(151) Sinha, K.; Wang, W.; Winey, K. I.; Maranas, J. K. *Macromolecules* **2012**, *45*, 4354−4362.
(152) Tudryn, G. J.; OReilly, M. V.; Dou, S.; King, D. R.; Winey, K. I.; Runt, J.; Colby, R. H. *Macromolecules* **2012**, *45*, 3962−3973.
(153) Bouchet, R.; Maria, S.; Meziane, R.; Aboulaich, A.; Lienafa, L.; Bonnet, J.; Phan, T. N. T.; Bertin, D.; Gigmes, D.; Devaux, D.; Denoyel, R.; Armand, M. *Nat. Mater.* **2013**, *12*, 452−457.
(154) Logan, B. E.; Rabaey, K. *Science* **2012**, *337*, 686−689.
(155) Kim, Y.; Hatzell, M. C.; Hutchinson, A. J.; Logan, B. E. *Energy Environ. Sci.* **2011**, *4*, 4662−4667.
(156) Logan, B. E.; Elimelech, M. *Nature* **2012**, *488*, 313−319.
(157) Saito, T.; Merrill, M. D.; Watson, V. J.; Logan, B. E.; Hickner, M. A. *Electrochim. Acta* **2010**, *55*, 3398−3403.
(158) Listorti, A.; Durrant, J.; Barber, J. *Nat. Mater.* **2009**, *8*, 929−930.
(159) Lewis, N. S.; Nocera, D. G. *Proc. Natl. Acad. Sci. U. S. A.* **2006**, *103*, 15729−15735.
(160) Miyatake, K.; Chikashige, Y.; Higuchi, E.; Watanabe, M. *J. Am. Chem. Soc.* **2007**, *129*, 3879−3887.
(161) Wu, S.; Qiu, Z.; Zhang, S.; Yang, X.; Yang, F.; Li, Z. *Polymer* **2006**, *47*, 6993−7000.
(162) Nuñez, S. A.; Hickner, M. A. *ACS Macro Lett.* **2013**, *2*, 49−52.
(163) Arges, C. G.; Ramani, V. *Proc. Natl. Acad. Sci. U. S. A.* **2013**, *110*, 2490−2495.
(164) Edson, J. B.; Macomber, C. S.; Pivovar, B.; Boncella, M. S. *J. Membr. Sci.* **2012**, *399- 400*, 49−59.
(165) Hibbs, M. R.; Fujimoto, C. H.; Cornelius, C. J. *Macromolecules* **2009**, *42*, 8316−8321.
(166) Hibbs, M. R. *J. Polym. Sci., Part B: Polym. Phys.* **2012**, in press. DOI: 10.1002/polb.23149.
(167) Zhang, Z.; Wu, L.; Varcoe, J.; Li, C.; Ong, A.; Poynton, S.; Xu, T. *J. Mater. Chem. A* **2013**, *1*, 2595−2601.
(168) Kim, D. S.; Labouriau, A.; Guiver, M. D.; Kim, Y. S. *Chem. Mater.* **2011**, *23*, 3795−3797.
(169) Noonan, K. J. T.; Hugar, K. M.; Kostalik, H. A.; Lobkovsky, E. B.; Abruña, H. D.; Coates, G. W. *J. Am. Chem. Soc.* **2012**, *134*, 18161−18164.